10-12-2010

Osteology, Natural History Notes, and Phylogenetic Relationships of the Poorly Known Caribbean Frog *Leptodactylus nesiotus* (Anura, Leptodactylidae)

María Laura Ponssa

Michael J. Jowers

Rafael O. de Sá
University of Richmond, rdesa@richmond.edu

Zootaxa 2646: 1–25 (2010)
www.mapress.com/zootaxa/

Article

ISSN 1175-5326 (print edition)
ZOOTAXA
ISSN 1175-5334 (online edition)

Osteology, natural history notes, and phylogenetic relationships of the poorly known Caribbean frog *Leptodactylus nesiotus* (Anura, Leptodactylidae)

MARÍA LAURA PONSSA[1], MICHAEL J. JOWERS[2], & RAFAEL O. DE SÁ[3]

[1]*CONICET. Fundación Miguel Lillo, San Miguel de Tucumán, Tucumán, Argentina. E-mail: mlponssa@hotmail.com.ar*
[2]*Division of Ecology and Evolutionary Biology, Institute of Biomedical and Life Sciences, University of Glasgow, Glasgow, UK. E-mail: michaeljowers@hotmail.com*
[3]*Department of Biology, University of Richmond, Richmond, Virginia, 23173, US. E-mail: rdesa@richmond.edu*

Abstract

The *Leptodactylus melanonotus* group consists of 15 species, but references to skeletal characters are available for only three species: *L. leptodactyloides, L. melanonotus, and L. diedrus*. *Leptodactylus nesiotus* is a member of the *melanonotus* group known only from the type locality, Bonasse swamp, on the Southwestern peninsula of Trinidad, Trinidad and Tobago. This species has been categorized as vulnerable given its restricted distribution. Herein, we report the adult osteology of *L. nesiotus*, the skeletal characters are compared with the available data from other *Leptodactylus* species. A phylogenetic analysis recovers a paraphyletic *L. melanonotus* group relative to the *L. latrans* group. A monophyletic "*latrans-melanonotus*" clade is supported by five synapomorphies. *L. nesiotus* is recovered as the sister species of *L. validus*, a relationship supported by two synapomorphies: T-shaped terminal phalanges and a dark-colored stripe on the outer surface of arm. In addition, we report on the ecology of this poorly known species.

Key words: skeleton, ecology, phylogenetic relationships, *Leptodactylus nesiotus*

Resumen

El grupo *L. melanonotus* del género *Leptodactylus* incluye 15 especies, aunque sólo existen reportes de caracteres osteológicos para tres de ellas: *L. leptodactyloides*, *L. melanonotus* y *L. diedrus. Leptodactylus nesiotus* es un miembro del grupo *L. melanonotus* que ha sido categorizado como vulnerable debido a su distribución restringida, ya que es conocido sólo de la localidad tipo: La ciénaga de Bonasse, sudoeste de la península de la isla Trinidad, Trinidad y Tobago. En este trabajo se aportan datos sobre la osteología de adultos de *L. nesiotus*, los cuales son comparados con lo observado en otras especies del género, y se sumaron a una matriz previamente elaborada. Esta fuente de caracteres se utilizó para realizar un análisis de parsimonia y proponer una hipótesis filogenética. El grupo *L. melanonotus* resultó parafilético respecto al grupo *L. latrans*. El clado *latrans-melanonotus* es apoyado por cinco sinapomorfías. Se infiere a *Leptodactylus nesiotus* como la especie hermana de *L. validus*, relación apoyada por dos sinapomorfías: falanges terminales en forma de T, y presencia de banda oscura en el borde externo del brazo. Además se reportan observaciones sobre la ecología de esta especie pobremente conocida.

Introduction

The genus *Leptodactylus* (Fitzinger 1826) consists of 87 species (Frost 2009) that have been traditionally clustered into five species groups *Leptodactylus fuscus*, *Leptodactylus melanonotus*, *Leptodactylus latrans*, *Leptodactylus pentadactylus*, and *Leptodactylus marmoratus* (Heyer 1969a). Phylogenetic studies of the genus have been limited, only including a few species of each group (Maxson & Heyer 1988; Heyer 1998; Larson & de Sá 1998; de Sá, Heyer & Camargo 2005; Heyer *et al*. 2005) or focusing on a single group (Ponssa 2008). *Leptodactylus nesiotus* (Heyer 1994) is currently considered a member of the *L. melanonotus* group. This species has been categorized as vulnerable given its restricted distribution, known only from the

Accepted by M. Vences: 9 Sep. 2010; published: 14 Oct. 2010

type locality, in the Bonasse Swamp on the southwestern peninsula of Trinidad, Trinidad and Tobago (IUCN 2006).

Osteology has been traditionally and widely used in amphibian phylogenetic studies. References to skeletal features and osteological characters of *Leptodactylus* are available for: *L. chaquensis* (Heyer 1998; Perotti 2001), *L. insularum* (Heyer 1998), *L. laticeps* (Ponssa 2006), *L. pentadactylus* (Heyer 1969b; Heyer 1998), *L. riveroi* (Heyer 1998), *L. lauramiriamae* (Heyer & Crombie 2005), *L. silvanimbus* (Heyer 1998), species of the *L. fuscus* group (Heyer 1998; Ponssa & Lavilla 1998; Ponssa 2008), species of the subgenus *Lithodytes* (Heyer 1974; 1998; Ponssa & Heyer 2007), and for the *Leptodactylus* genus in general (Lynch 1971). Among the 15 species in the *L. melanonotus* group, osteological characters have been previously reported only for *L. leptodactyloides*, *L. melanonotus*, and *L. diedrus* (Heyer 1998).

Osteological characters within this group are useful for species diagnoses, to understand patterns of morphological evolution, and can contribute to assess phylogenetic relationships. Herein, we report on the adult osteology of *L. nesiotus* and compare it with other available data for the genus. A phylogenetic analysis was performed to assess the relationships of this species to other *Leptodactylus* species and to test the monophyly of the traditional *L. melanonotus* species group. Furthermore, we report observations on the ecology and natural history of this poorly known species.

Material and methods

Three *Leptodactylus nesiotus* males and one female (N = 4) were collected at Bonasse swamp (10°05'41.55"N, 61°49'53.35"W; 10 m.s.n.m.), Trinidad (Trinidad and Tobago), on July 3, 2004, by M. J. Jowers and R. Campbell-Palmer. The specimens were taken to the laboratory for further observations. They were housed in tanks (0.95 cm x 35 cm x 35 cm) with a central mud islet with plenty of shrub branches, wood, few stones, leaf litter, and water to best resemble their natural habitat. The swamp is easily accessed through the Southern Main road that divides the swamp into two separate areas. To the Northern side of the road, the swamp reaches its maximum water capacity, about a meter deep. Here, the swamp (about half a hectare) is composed of few tall trees growing in the water and smaller trees on islet formations found around the back and centre of the swamp. The swamp is surrounded by tall reeves growing at the side of the road on the Northern section. The Southern side of the swamp is more open and resembles a field of tall grasses after a heavy rainfall. The water rarely reaches more than a foot in depth and the area was occasionally dry. Frogs were not heard calling and thus surveys were not carried out in this area.

For the morphological analysis two *Leptodactylus nesiotus* specimens, a female (USNM 558322) and a male (USNM 558321) were cleared and double stained following Wassersug's (1976) protocol. Skull measurements were taken with Image Tool software (Fig. 1). The terminology for cranial and postcranial osteology follows Trueb (1973; 1993) and Trueb *et al.* (2000). Terminology of digits and carpal osteology follows Fabrezi (1992), olfactory region follows that of Pugener and Maglia (2007) and Maglia *et al.* (2007), laryngeal morphology follows Trewavas (1933), and sesamoids terminology follows Ponssa *et al.* (2010). Fingers are numbered II–V following Fabrezi and Alberch (1996). Osteological data of species of the *L. fuscus* group follows Ponssa (2008) whereas data for *L. colombiensis*, *L. melanonotus*, *L. validus*, and *L. silvanimbus* (species in the *L. melanonotus* species group) follow Heyer (1998) and Ponssa (2008). The osteology of *L. laticeps* was included as a representative species of the *L. pentadactylus* group (Ponssa 2006). Herein, the *L. latrans* group refers to the traditionally known *L. ocellatus* group, following Lavilla *et al.* (2010).

Characters that resulted from the description were coded and combined with those previously published for the *Leptodactylus fuscus* group (Ponssa 2008) (Appendix 1).

A maximum parsimony (MP) analysis (i.e., traditional search, with 2000 different addition sequences to the tree bisection-reconnection branch swapping method (TBR), retaining 100 trees per replication; internal branches were considered unsupported and collapsed during searches if any possible states were shared between ancestor and descendent nodes -min. length = 0 option-) was performed in TNT (Goloboff *et al.*

2003a). The analysis was made under implied weighting (Goloboff 1993), an improvement over the successive weighting method (Farris 1969) implemented in Hennig86 (Farris 1988), which is designed to down-weight homoplasy. The fit of each character is calculated with a concave function of its number of extra steps (i. e., more homoplasy, less fit); the preferred tree maximizes the total fit. The down weighting strength is determined by modifying a concavity constant (K); the data set was analyzed with K = 3. The multistate characters which states follow a logical sequence were considered to be additive; the addition in this case only reflects degrees of similarity and is independent of any consideration on the sequence in which the characters evolved (Lipscomb 1992; Goloboff 1997). Nodal support was calculated with symmetric resampling (2000 replicates, with 10 addition sequences, saving up to 100 trees each). This method is a resampling technique (as bootstrap and Jacknife) not distorted by weight or costs. The results are expressed as values of GC (groups present/contradicted), with a change probability of 0.33 (Goloboff *et al*. 2003b). The GC values consist in the difference between the frequency of the considered group and its contradictory more frequent group. The values of GC are from -100 (maximum contradiction), passing by 0 (indifference), to 100 (maximum support) (Goloboff *et al*. 2003b). Relative bremer support (Goloboff and Farris 2001) was also performed retaining up to 6000 trees in the searches, suboptimal in fit values between 1 and 4, TBR swapping starting from the optimal tree.

Results

Natural history. The elusive behavior of this species made its identification and capture in the field extremely difficult. Despite acoustic identification of *Leptodactylus nesiotus* males (approx. N = 10) during several visits to the swamp throughout the wet season of 2002 and 2003 (by several research groups), all our surveys previous to 2004 resulted in no sightings or captures. During early summer (May–June), males could be heard calling between the thick reeves, mostly at the back of the Northern side of the swamp. The tall and dense vegetation made progress difficult and noisy; thus, males would stop calling and could not be located. Furthermore, frogs would hide throughout the dense stagnant brackish water at the base of the reeves. On the other hand, throughout the wet months of July and August, swamp depth reached approximately a meter in depth and lack of vegetation throughout the middle section of the swamp made the calling males very conspicuous.

The swamp area was surveyed for the presence of *Leptodactylus nesiotus* by visual and acoustic inspection. All captured males were heard calling (the female was seen moving) in the centre of the swamp, not far from the road, approximately 40–50 meters away, and in close proximity to or on small islet formations in the middle of the swamp. These islets (approx. length 2–3 m, width 1.5–2 m) were shaded by one or more trees with aerial roots creating a network of small crevices and holes through the muddy soil, mostly covered by leaf litter. *L. nesiotus* were heard calling outside the burrows that seemed to have been dug in the mud close to the tree roots.

On the early attempts to approach calling males, they would stop calling and would not recommence for several minutes. Furthermore, when frogs were disturbed they would hide inside a burrow. No male frogs were observed swimming or floating on the water. The position of calling males were only revealed immediately after approaching them when the specimens were disturbed by our presence; as they tried to hide they created visible water movement. All specimens were hand caught by feeling for them in the burrows immediately after they hid into them. Most of the burrows were less than half a meter deep with its opening slightly above water level and were thus partially filled with water and mud. Some burrows seemed to connect with others, leading towards the centre of the islet, just under the surface, but this could not be corroborated.

There is currently no information available on the nesting or larvae biology of this species. We inspected the entire swamp in all our visits for foam nests and/or larvae; all searches among the vegetation (i.e., between reeves, trees, grasses, and other plants), floating on the water surface, or by digging in the swamp banks or in the swamp islets where the specimens had been captured proved to be unsuccessful. Nest searching took place on several occasions from May to September, during drier periods when there was little water and when the

swamp was at its highest water capacity. Sampling for tadpoles with large hand nets throughout all the areas of the swamp also proved unsuccessful.

The elusive field behavior of *L. nesiotus* was also observed in the laboratory. On the rare occasions that the frogs left their cover, and were thereafter distressed by our presence, they would immediately retreat to their shelter and were not observed swimming or exposed outside their shelter. The males would call mostly during the afternoon hours. As in the field, calling did not seem to be simultaneous or synchronized, thus when a male finished calling, another frog would start calling or would arrange the call bout during other males interbouts. Males were heard calling occasionally late in the afternoon.

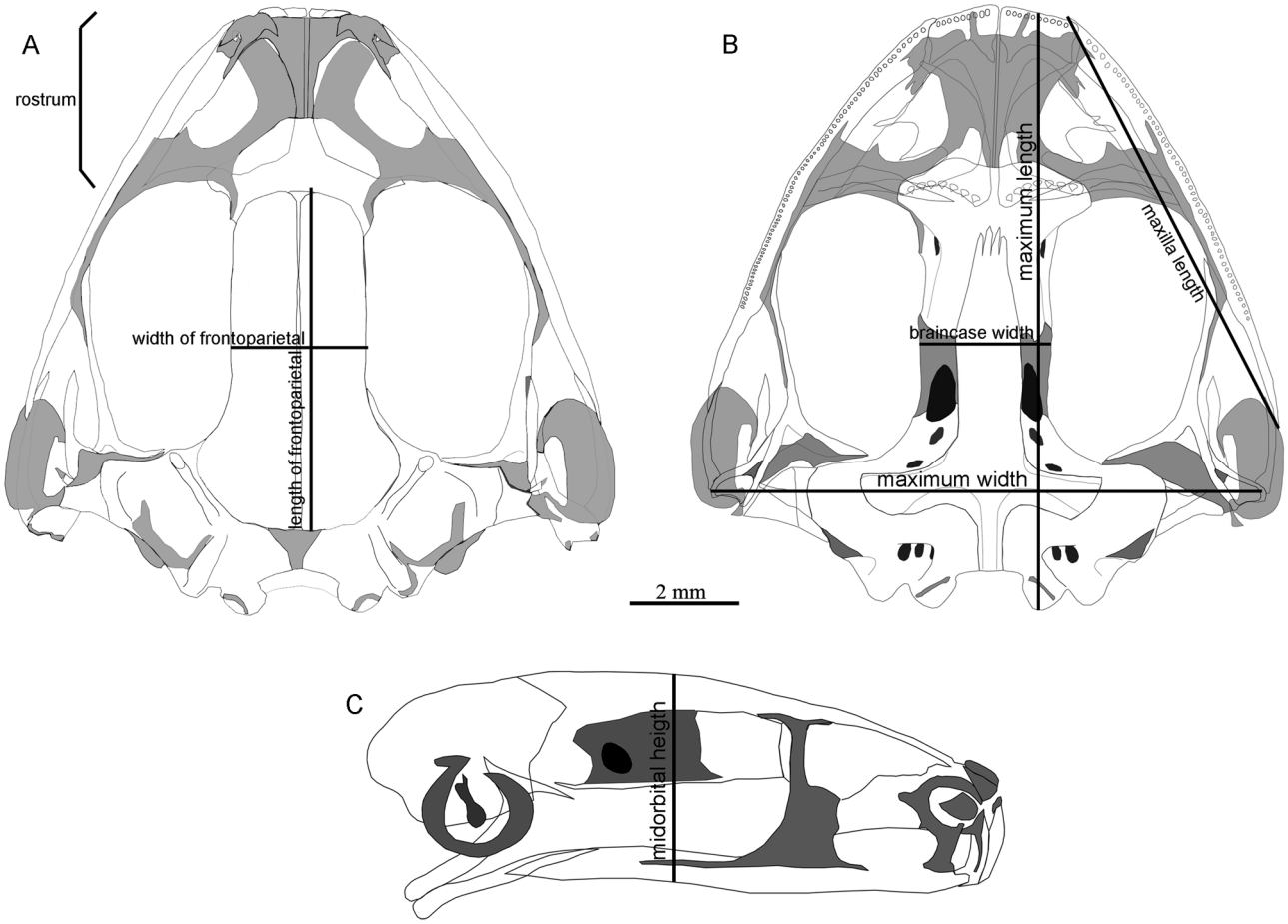

FIGURE 1. Graphical representation of skull showing the dimensions measured. (A) dorsal, (B) ventral and (C) lateral views.

Osteological description

Cranium

(Fig. 2 and 3)

The skull is widest at the level of the articulation of the maxilla with the quadratojugal; its maximum width is about equal to the maximum length (length/width = 0.96). The rostrum is short, representing less than a quarter of the maximum length of the skull. The braincase is moderately broad; at the level of the midorbit, the width of the braincase is 24% of the greatest width of the skull. The midorbital height of the skull is 41.7% of the skull maximum length.

Mandible. The mandible is slightly curved in the prearticular region (Fig. 4). The mentomeckelians are L-shaped narrowly separated medially; with their shorter rami perpendicular to the horizontal plane of the skull.

The anterolateral margin of the mandible consists of a narrow dentary, which lacks odontoids or serrations and laterally overlaps Meckel's cartilage. The angulosplenial is the largest mandibular bone extending over 90% of the mandible, overlying the inner surface of Meckel's cartilage, and separated from the mentomeckelian bone by a space shorter than the length of the latter. Posteriorly, the angulosplenial bears the point of articulation, either cartilaginous or ossified, with the braincase and surrounds Meckel's cartilage through most of its length, except anteriorly where it only overlaps the medial margin of the Meckel's cartilage. The coronoid process is overall trapezoidal in shape and normally developed.

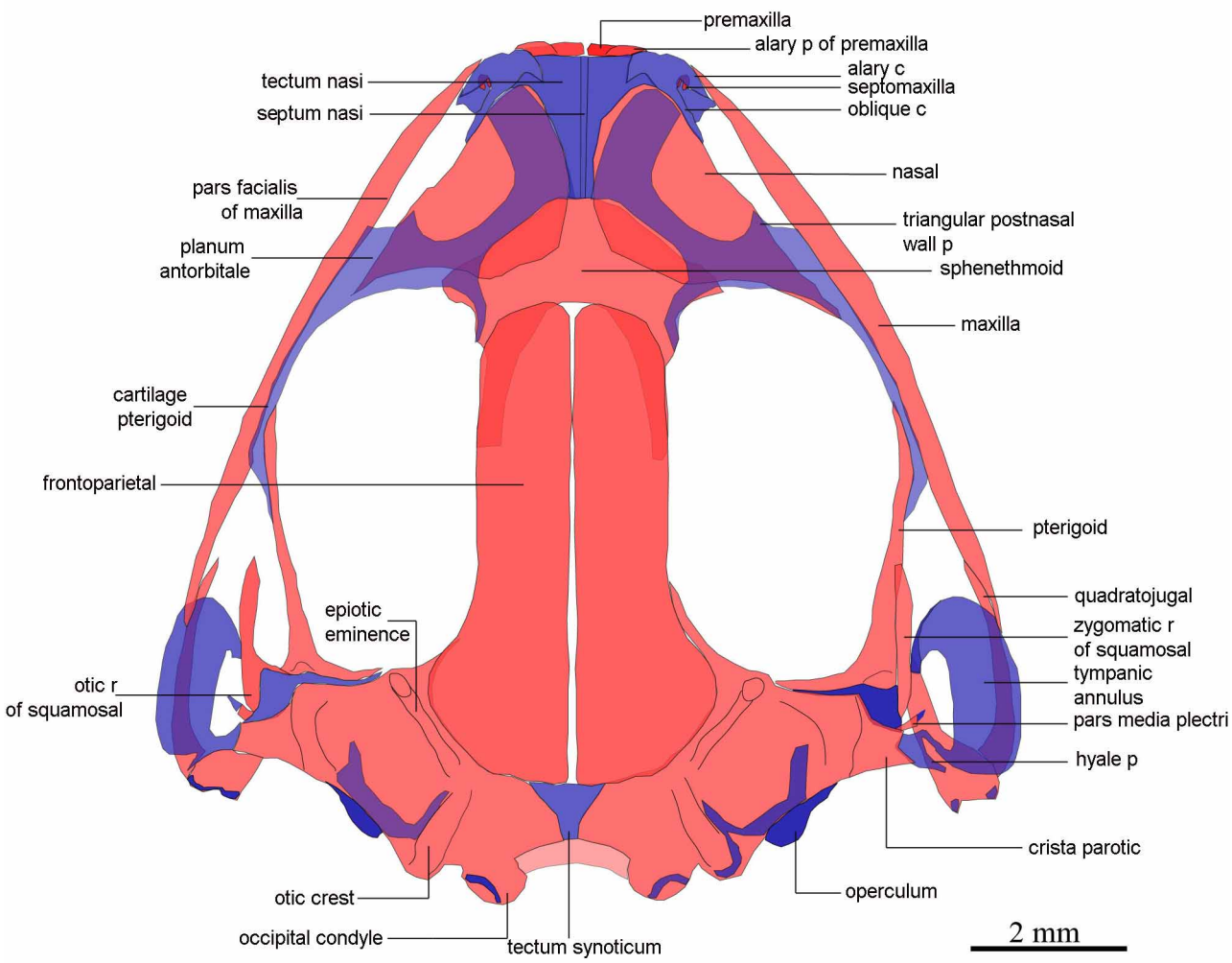

FIGURE 2. Skull of *Leptodactylus nesiotus*, dorsal view of the male specimen. c: cartilage; p: process; r: ramus.

Maxillary Arcade (Fig. 2 and 3). The upper jaw is complete and consists of the premaxilla, maxilla, and quadratojugal. Bicuspid and conical teeth with blunt tips are distributed on almost the complete maxillary arcade, except on its posterior 1/5. Each premaxilla bears 11 or 12 teeth and each maxilla has 56 to 59 teeth. The medial sides of the paired premaxillae are narrowly separated from one another. The *pars palatina* of the premaxilla articulate with the *pars palatina* of the adjacent maxilla. The alary processes are overall rectangular and perpendicular to the longitudinal axis of the skull; they are oriented dorsally and curved backwards; their medial edges are initially parallel to each other and slightly diverging dorsally. The *pars palatina* of the premaxilla bears medially a triangular palatine process; this process is bifid, with the inner ramus shorter than the outer one. The maxilla is elongated and represents 84.5% of the cranial length. Anteriorly, it bears a ventrolateral process that juxtaposes with the premaxilla; its posterior half is medially flat, corresponding to the surface of articulation with the anterior ramus of the pterygoid. Posteriorly, it overlaps the anterior tip of the quadratojugal. The height of the *pars facialis* of the maxilla commensurate with the alary processes of the premaxillae; posteriorly it ends anteriorly or at the level of the neopalatines, it

does not contact with the nasals. The *pars facialis* is well developed, lacks pre- and postorbital processes, and extends for approximately less than half the length of the maxilla.

The quadratojugals are rod-shaped, slender, and well-ossified bones. Posteriorly, each quadratojugal articulates with the ventral ramus of the squamosal.

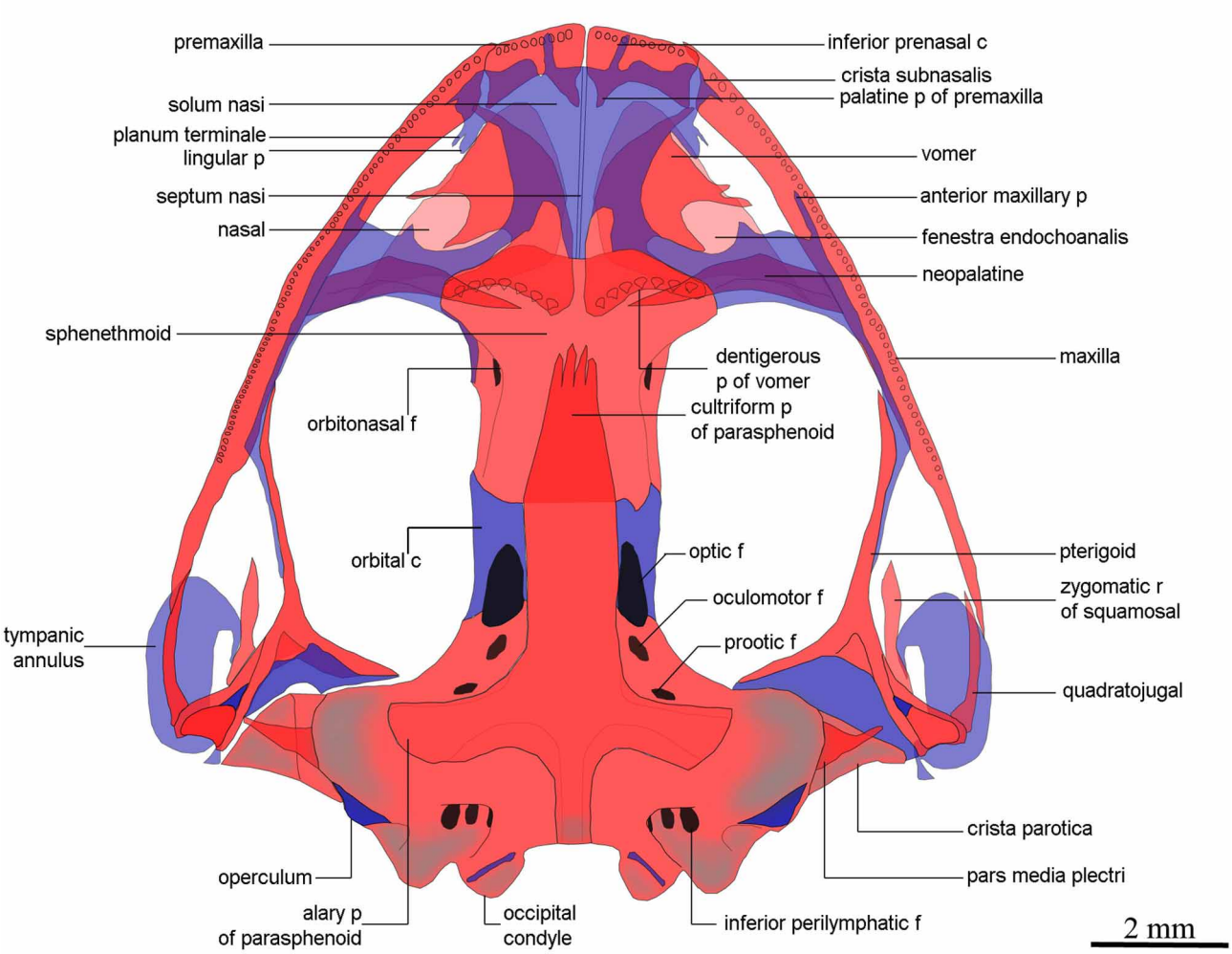

FIGURE 3. Skull of *Leptodactylus nesiotus*, ventral view of the male specimen. c: cartilage; f: foramen; p: process; r: ramus.

Neurocranium. The anterior neurocranium consists of the large olfactory capsules and the unossified anterior wall of the braincase. The medial walls of the nasal capsules are narrowly separated by a thin cartilaginous plate, the septum nasi. The nasal septum, as well as the *tectum* and the *solum nasi*, can be slightly mineralized.

A minute U-shaped septomaxilla is present, but obscured by the cartilages of the anterior nasal capsule. The posterior wall of the nasal capsule is formed by the *planum antorbitale*, a thick transverse wall of cartilage that is located between the braincase and the maxilla and forms the anterior edge of the orbital space (Fig. 2 and 3). Ventrally, the *planum antorbitale* is overlied by a simple neopalatine. The cartilaginous nasal roof, *tectum nasi*, is exposed between the nasal bones; it is anteriorly straight and extends to the level of the premaxillae. In dorsal view, the oblique cartilage, a short bar that extends from the nasal roof posterolaterally over the top of the nasal capsule, borders the anterior edge of the nasals. The ventrolateral portion of the oblique cartilage, the *planum terminale*, is a vertical plate of cartilage that forms the lateral wall of the nasal capsule. The inferior edge of the *planum terminale* has a posterior, rod-shaped, lingular process. The alary cartilage is located ventrally to the oblique cartilage. A poorly developed anterior maxillary process projects forward, from the anterior border of the *planum antorbitale*, and overlaps the inferior margin of the medial

surface the *pars facialis* of the maxilla. The posterior maxillary process extends from the posteroventral margin of the *planum antorbitale* to merge with the anterior ramus of the pterygoid, forming a single rod of cartilage that extends through the posterior ramus of the pterygoid.

Endochondral Braincase (Fig. 2 and 3). The endochondral braincase consists of three pairs of replacement bones — sphenethmoid, prootics, and exoccipitals — that are partially covered by the frontoparietals dorsally and the parasphenoid ventrally. The anterior margin of the bony sphenethmoid lies before the level of the *planum antorbitale* and its posterior margin reaches the midlevel of the orbit. The sphenethmoid forms the floor and the anterolateral walls of the braincase. The sphenethmoid is dorsally visible in the space between the nasals and frontoparietals. Its ventral face overlaps the medial tip of the neopalatines. There is a moderately broad orbital cartilage between the sphenethmoid and prootic, within which the optic foramina lies (Fig. 3). The optic foramen is bordered by the parasphenoid, prootic, and orbital cartilage, or only by the orbital cartilage and the parasphenoid. The posterior region of the braincase consists of the prootics and exoccipitals, each of which also contributes to the otic capsules. The anterior half of the frontoparietals overlaps the sphenethmoid. Ventrally, the vomers overlap the sphenethmoid. The orbitonasal foramen is visible, anterodorsal, and enclosed by the sphenethmoid.

The prootics form the margin of the prootic and oculomotor foramina, the posterolateral walls of the braincase, and all but the posteromedial portions of the otic capsules (Fig. 2). Dorsally, the posterior portion of the frontoparietal overlies the prootic.

Ventrally, the prootics are underlied by the parasphenoid anteromedially. They lack dorsal ornamentation, although a distinct epiotic eminence is visible on the median surface of each otic capsule. There is an enclosed occipital canal.

The exoccipitals form the posteromedial walls of the otic capsules, the margins of the foramen magnum, and the occipital condyles (Fig. 3). Ventromedially, the exoccipitals are partially overlaped by the posteromedial processes of the parasphenoid. Dorsally, each exoccipital bears a well-developed occipital crest. The occipital condyles have moderately distinct stalks and have curved articular surfaces that face posteromedially; they are widely separated and shaped as half-moons. The otic capsule is variably ossified in the region of the inner ear and bears a moderately broad crista parotica that bridges the tympanic cavity from the prootic to the short otic ramus of the squamosal. The epiotic eminences are shallow and dorsally overlaped by the posterolateral margin of the frontoparietal. The anterior eminence is slightly longer than the posterior and the angle between both arms is approximately 90°. The occipital condyles are behind the level of the posterior edges of the quadrates. The jugular foramen opens in the posterior wall of the otic capsule, lateral to the occipital condyle.

Plectral Apparatus. The tympanum is supported by the tympanic annulus, which lies below the otic ramus and joins with the crista parotica behind the ventral ramus of the squamosal. The tympanic annulus is incomplete dorsally (Fig. 2). The *pars externa plectri* is cartilaginous, approximately globe-shaped, with a knob-like process distally and two slender tips proximately; it is almost half the length of the stapes (*partes interna* and *media plectri*) and lies internal to the tympanic annulus. The *pars media plectri* is a long, slender, slightly curved, and ossified stylus; it is fused synostotically with the *pars interna plectri*, which forms the basal plate of the stapes. The medial head of the *pars interna plectri* meets the *fenestra ovalis* anterodorsal to the operculum. The *pars interna plectri* is expanded and almost completely ossified except for its cartilaginous border. The operculum is a thin, externally convex cone that covers almost completely the oval window; it is cartilaginous with some mineralization. The opercular crest is well developed.

Dermal Investing Bones. The triangular and paired nasals roof the nasal capsules. They are medially separated and have curved borders (Fig. 2). The maxillary processes are well developed; they have sharp ends and straight borders, and extend posterolaterally without reaching the maxilla. Posteromedially, the nasals invest the anterior margin of sphenethmoid and do not contact with the frontoparietals. The anterior margin of the nasals projects anteriorly and dorsally overlaps the nasal cartilages; their anterolateral border is slightly concave.

The paired frontoparietals have a width of 42.3% of their length, and their length is 56.6% of the skull length (Fig. 2). The external borders are slightly convex. The posterior portion is expanded and rounded. The

posterior one-fifth of the frontoparietal dorsally overlaps the medial margins of the epiotic eminences and the anterior half of the dorsomedial prootics. They do not reach the foramen magnum. Anteriorly, the frontoparietals dorsally overlap the sphenethmoid to the level of the superciliary cartilages; their lateral margins are not fused with the prootics. The frontoparietals are adjacent to each other medially throughout of their lengths and completely cover the frontoparietal fenestra.

Each *lamina perpendicularis* projects ventrally to form the dorsomedial margins of the orbit. Anteriorly, the *lamina perpendicularis* overlaps the posterolateral surface of the sphenethmoid, whereas posteriorly it articulates with the anterior edge of the prootic.

The parasphenoid is T-shaped, unornamented, and bears a prominent, posteromedial process that terminates at the margin of the foramen magnum. This bone is not fused with the underlying bones. The cultriform process does not reach the neopalatines and its lateral margins are convex. The process is narrow posteriorly, wider near the anterior margin of the optic foramen, and its margins converge gradually anteriorly. The anterior half of the cultriform process ventrally covers the posterior two-third of the sphenethmoid. The alary processes ventrally overlap the otic capsules. They do not reach the prootic-pterygoid articulation. The *alae* are moderately long (their length about equal to the width of the cultriform process), posterolaterally oriented, and distally expanded and rounded.

The neopalatines (Fig. 3) are slender, curved, and posteriorly concave bones; their edges are sharp without odontoids but a medial ridge extends along its length. The neopalatines are widest medially. One-third of its medial length articulates with the lateral margin of the sphenethmoid, anteriorly to the orbitonasal foramen. The lateral tips of the neopalatines are underlied by the *planum antorbitale* and contact the *pars palatina* of the maxilla. The acuminate medial tips do not contact medially. The vomers cover the medial tips of the neopalatines.

The vomers are paired, moderate-sized, and dentigerous dermal elements that are associated with the anterior margin of the sphenethmoid in the palate (Fig. 3). They do not contact medially with each other. Each vomer consists of an arcuate bone that anteriorly borders the posterior margins of the choana. The anterior ramus is shorter than the middle ramus, whereas the latter is longer than the posterior ramus. The angle between the anterior and middle rami is approximately 90º; whereas the angle between the middle and posterior rami is less than 90º. Each dentigerous process bears a horizontal series of 11–12 teeth. The tip of the anterior ala is spine-like and contacts with the premaxilla–maxilla articulation. The vomers articulate posteriorly with the neopalatines.

Suspensorium. Each pterygoid possesses well developed anterior, medial, and posterior rami (Fig. 2 and 3). The anterior ramus anteriorly diverges to the midline of the skull and articulates with the medial surface of the maxilla at its midlength; it does not reach the neopalatines. The pterygoid is separated from the maxilla by the pterygoid cartilage, which lies along the medial margin of the maxilla in the orbital region. The medial ramus is shorter than the posterior ramus. The posterior ramus forms the otic plate and overlaps the anterolateral and ventral cartilaginous corner of the otic capsule. The medial ramus contacts the edge of the ossified lateral margin of the prootic. The posterior ramus is laminar and curved, its dorsal edge is in contact with the squamosal; posterolaterally, this ramus invests the medial surface of the *pars articularis* of the palatoquadrate. The anterior and posterior rami together have the shape of an elongated S.

The squamosal is T-shaped (Fig. 2). The zygomatic ramus is almost equal in length to the otic ramus, both are curved, concave medially, and with acuminate anterior tips. The ventral margin of the posterior portion of the zygomatic ramus forms the anterior and dorsal margins that support the tympanic annulus. The otic ramus almost articulates with the crista parotica, but it does not contact with the frontoparietal. The ventral ramus articulates with the quadratojugal. The tip of the ventral ramus is expanded, forming an angle greater than 45º with the horizontal plane of the skull. The angle between the squamosal and maxilla is less than 45º.

Hyoid apparatus. The width of the cartilaginous hyoid corpus is greater than its medial length, which is 84% of the width (Fig. 4). The hyoglossal sinus is broadly U-shaped. The hyoid plate is cartilaginous and mineralized at the base of the alary, hyale, posterolateral, and posteromedial processes. The margins are anteriorly and posteriorly slightly divergent. The hyales are thin, curved, and with a curvature at the level just behind of the alary processes. Short anteromedial processes are present. The anterolateral processes are

moderate and slightly oriented forward. The posterolateral processes are thin, broad based, and pointed distally. They arise on the posterolateral side of the hyoid plate and they are oriented postero-laterally; the posterior ends extend beyond the level of the posterior edge of the hyoid plate. The bony posteromedial processes are slightly expanded proximally and distally; the anterior ends are separated from one another; the posterior tips of these processes are cartilaginous. The posteromedial processes diverge laterally at 45° from the midline to support the laryngeal cartilages.

Laryngeal Apparatus (Fig. 4). The arytenoids consist of a pair of valve-shaped cartilages, triangular in lateral view. The cartilaginous cricoid forms a complete ring. An esophageal process is differentiated and triangular shaped. A thin bronchial process is differentiated. In females, the cricoid and the arytenoids are smaller than in males.

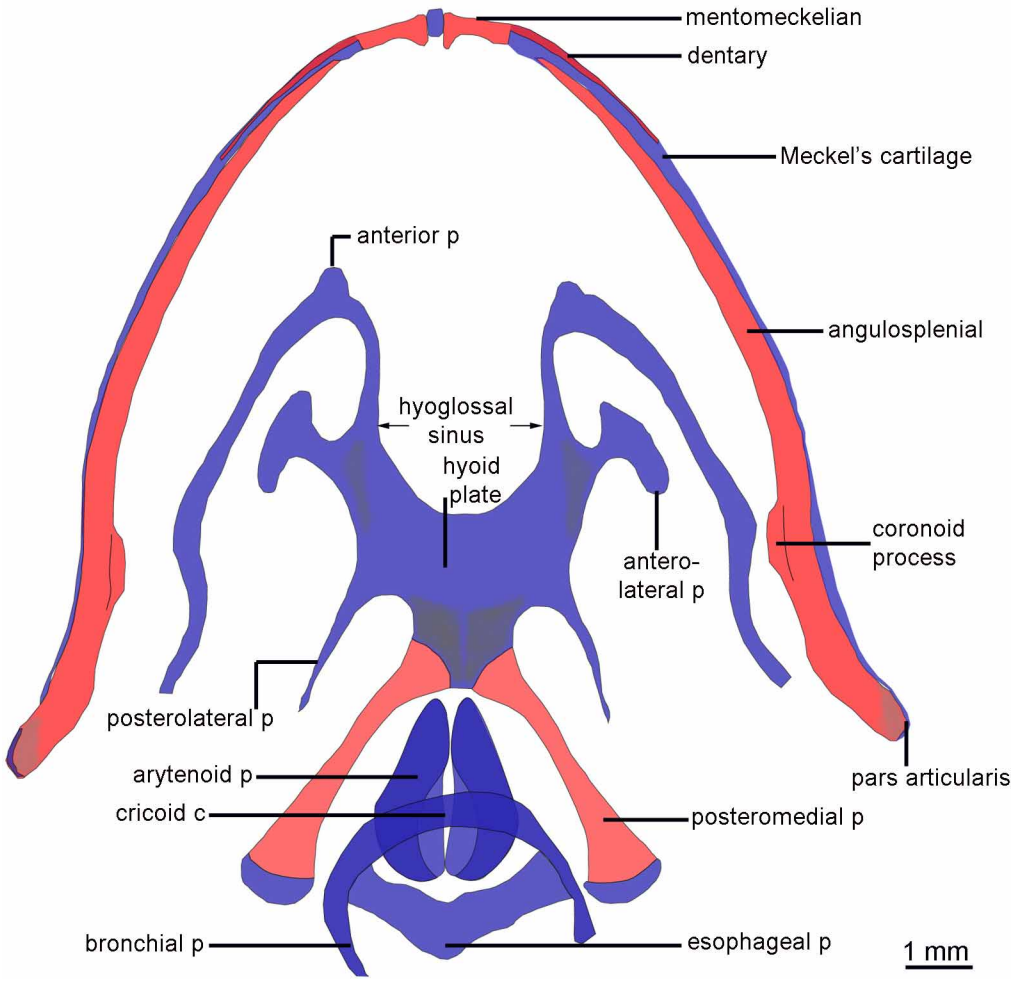

FIGURE 4. Hyoid of *Leptodactylus nesiotus*, male specimen. c: cartilage; p: process.

Postcranial osteology of Adults

*Axial skeleton***.** The vertebral column consists of eight procoelous presacral vertebrae, the sacral vertebra, and the urostyle (Fig. 5). The atlas is not fused to the adjacent vertebra; it is dorsally divided, with a groove dividing both halves. The cervical cotyles are bean-shaped, oblique, and characteristic of Type I (Lynch 1971). The intercotylar region is concave. In ventral view, the centrum of the atlas is wider than those of the other vertebrae. The neural arches of each vertebrae have well-developed dorsal ridges and a pair of parasagital processes extending laterally. The neural arches of vertebrae I–V are imbricated. The articular facets of the pre- and postzygapophyses are simple, lacking ridges or sulci. The lengths of the vertebral centra exhibit moderate differences that are most evident in ventral view. Presacral II is the shortest, presacral III is

slightly longer, and presacrals IV is slightly longer than the first two vertebrae. The remaining presacrals are almost equal in length. The relative lengths of the transverse processes in descending order are: III > IV ≈ V≈VI ≈ VII≈ VIII > II. The transverse processes of Vertebra III, VI, and VII are approximately perpendicular to the notochordal axis, whereas those of Vertebra IV–V are posterolaterally oriented and those of Vertebrae II and VIII are anteriorly directed. The scarcely dilated sacral diapophyses are ovoid in cross-section and are posteriorly oriented. The edges of the diapophyses are straight.

The urostyle is slender and not fused to the sacral vertebra; it is slightly shorter than the presacral length of the vertebral column. The bone has a bicondylar articulation with the sacrum and bears a dorsal crest throughout most of its length. The dorsal crest is highest anteriorly, diminishing in height posteriorly, and finish anteriorly with a knob. The ilio-sacral articulation is Type II B of Emerson (1982). There is a mineralized sesamoid element between the ilio-sacral articulations.

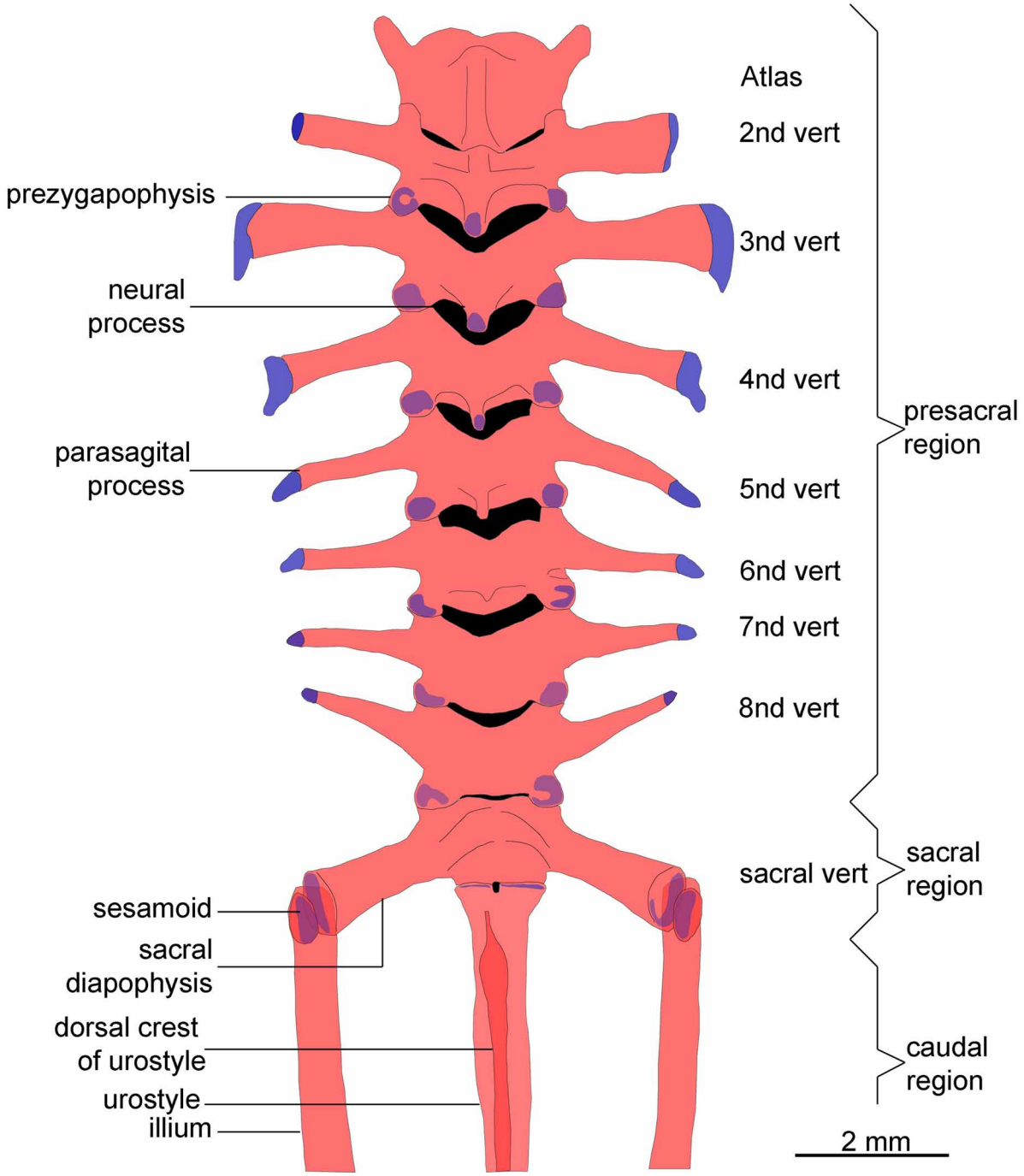

FIGURE 5. Vertebral column and pelvic girdle of *Leptodactylus nesiotus*, male specimen.

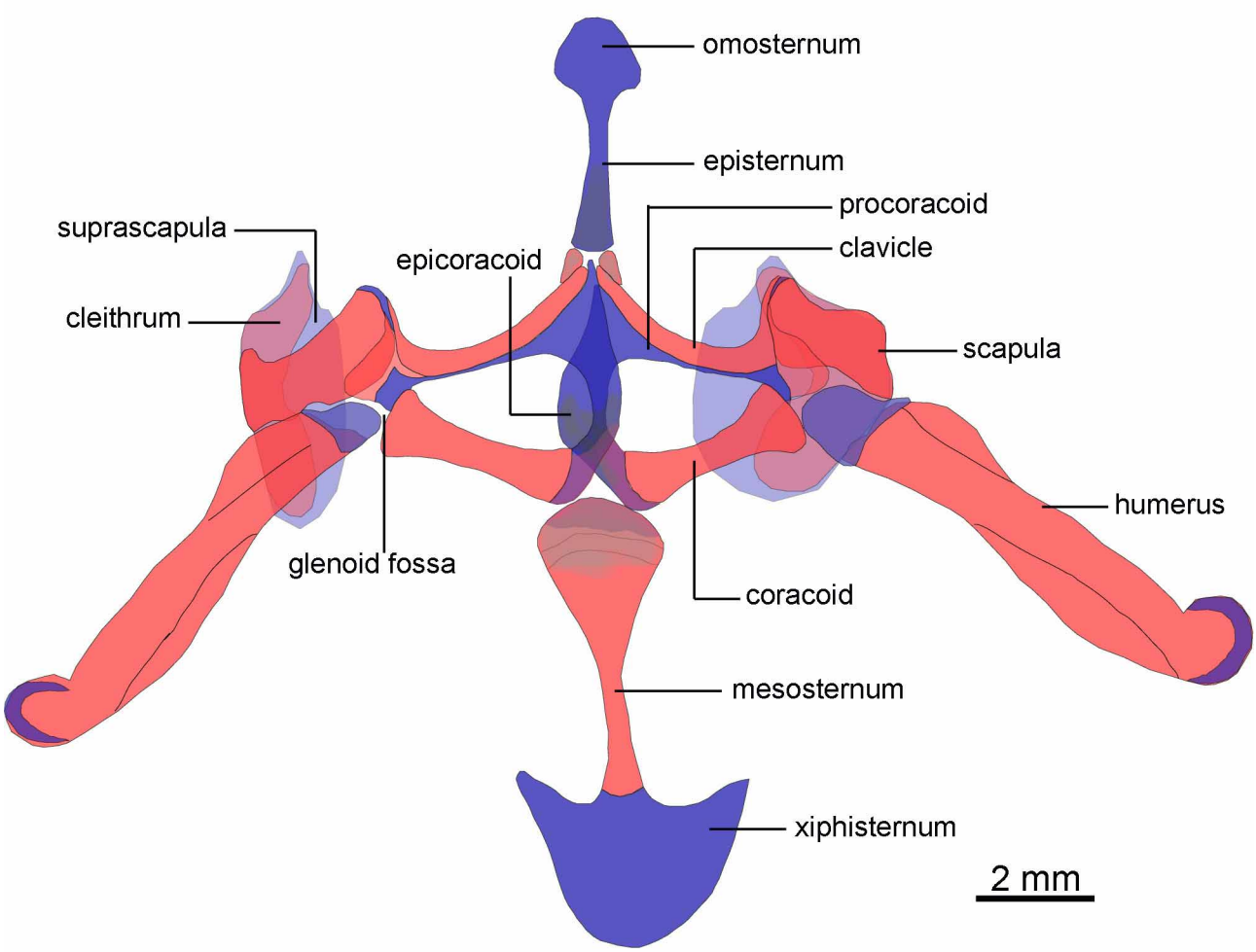

FIGURE 6. Pectoral girdle of *Leptodactylus nesiotus*, male specimen.

Pectoral girdle (Fig. 6). The girdle is arciferous. The omosternum is cartilaginous. The fan-shaped anterior expansion is shorter than the xiphisternum. The anterior margin of procoracoid extends to the level of the medial ends of the clavicles, separating the clavicles. This bone is synchondrotically united to the epicoracoid cartilages posteromedially. Each procoracoid cartilage extends laterally and posteriorly and contributes to the formation of the glenoid fossa. The procoracoids are slightly mineralizated. The pectoral fenestra is wider than long, teardrop-shaped, with its main axis transverse to the vertebral column. The inner edge is concave; the outer margin is extremely narrow. Each pectoral fenestra is anteriorly bordered by the procoracoid cartilage, medially by the epicoracoid cartilage, and posteriorly by the coracoid. The epicoracoid is an arcuate cartilage, with mineralized anterior and inner lateral edges. The episternum is cartilaginous and rod-like, slightly expanded and mineralizated posteriorly. The mesosternum is ossified with a cartilaginous anterior end. The xiphisternum is semicircular, anteriorly mineralizated, with two anterior prolongations in the lateral borders.

Each clavicle is curved, bow-shaped, and has concave anterior edges. The distal end of the clavicle is expanded dorsally into a wedge-shaped process that articulates with the *pars acromialis* of the scapula. The clavicles do not reach the glenoid fossa. The coracoid is subrectangular, stout, with the glenoidal and sternal ends almost equally expanded. The scapula is overall rectangular and almost equal in length to the coracoid. However, the width of the scapula is twice that of the coracoid. The anterodorsal portion of the scapula consists of a convex plate, the *pars acromialis*; whereas a posteriorly concave plate, the *pars glenoidalis*, forms the dorsolateral wall of the glenoid fossa. The prominent *pars acromialis*, clearly distinct from the *pars glenoidalis*. The glenoid cavity is bordered by the scapula and coracoid.

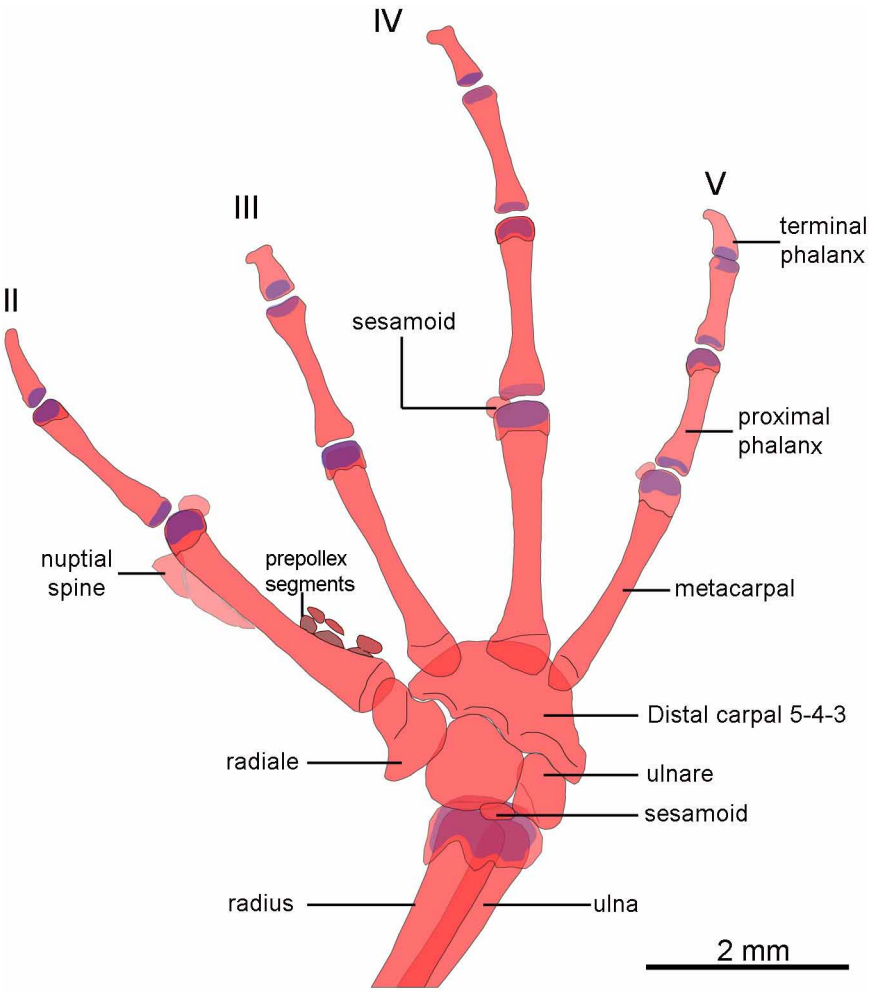

FIGURE 7. Right manus elements of *Leptodactylus nesiotus*, male specimen.

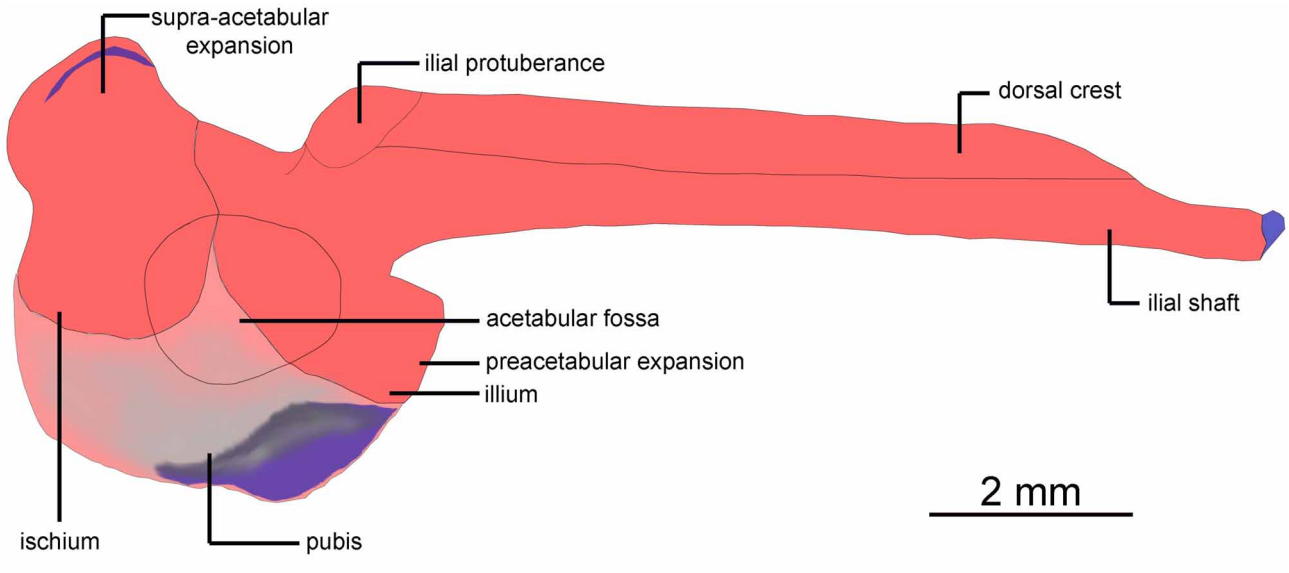

FIGURE 8. Pelvic girdle of *Leptodactylus nesiotus*, male specimen.

The cleithrum is an ossified, very thin, and bifid lamina; the posterior ramus is shorter or equal to the anterior ramus. On the anterior side it has a superficial ledge. The cleithrum overlaps most of the medial margin of the cartilaginous suprascapula and is continuous with the suprascapula. The suprascapula extends distally as a broad, flat blade, and possesses a small, anteriorly projected hook-shaped process.

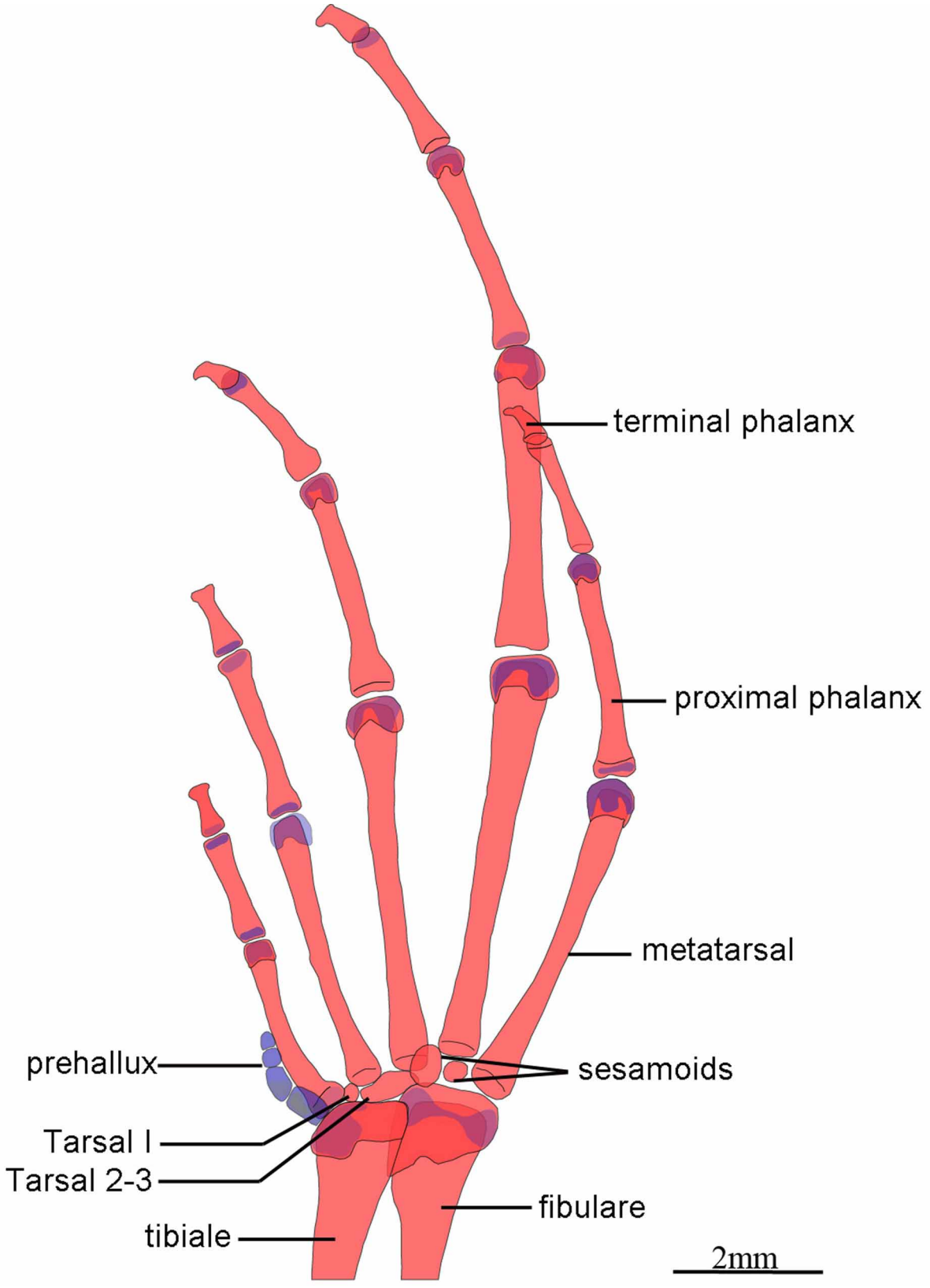

FIGURE 9. Right pes elements of *Leptodactylus nesiotus*, male specimen.

Forelimb and manus. The humerus bears a well-developed *crista ventralis* over half of its length (Fig. 6). The distal head (*eminentia capitata*) is broadly expanded; the glenoid head (*caput humeri*) is expanded, rounded, and almost equal in size to the *eminentia capitata*. The males bear a well-developed crest on the

distal two-third of the humerus. The radioulna is flattened; the *sulcus intermedius* is indicated by a distinct groove.

Five carpal elements are present, corresponding the Type E morphology (Fabrezi 1992): ulnare, radiale, element Y, Distal Carpal 5-4-3, Distal Carpal 2, and elements of the prepollex (Fig. 7). The phalangeal formula is 2–2–3–3. A rounded sesamoid cartilage is embedded in the tendons of the palmar surface, the palmar sesamoid. Dorsal to the articulation of the radioulna with radiale there is an additional small sesamoid, the pararadial. The terminal phalanges are T-shaped. A couple of small glide sesamoids are present on the ventral face of the distal epiphysis of the metacarpus. The males' inner metacarpus bears a nuptial spine. The prepollex, which also has a nuptial spine, consists of three elements in addition to the basal segment. There are three smaller segments beside each respective segment of the prepollex.

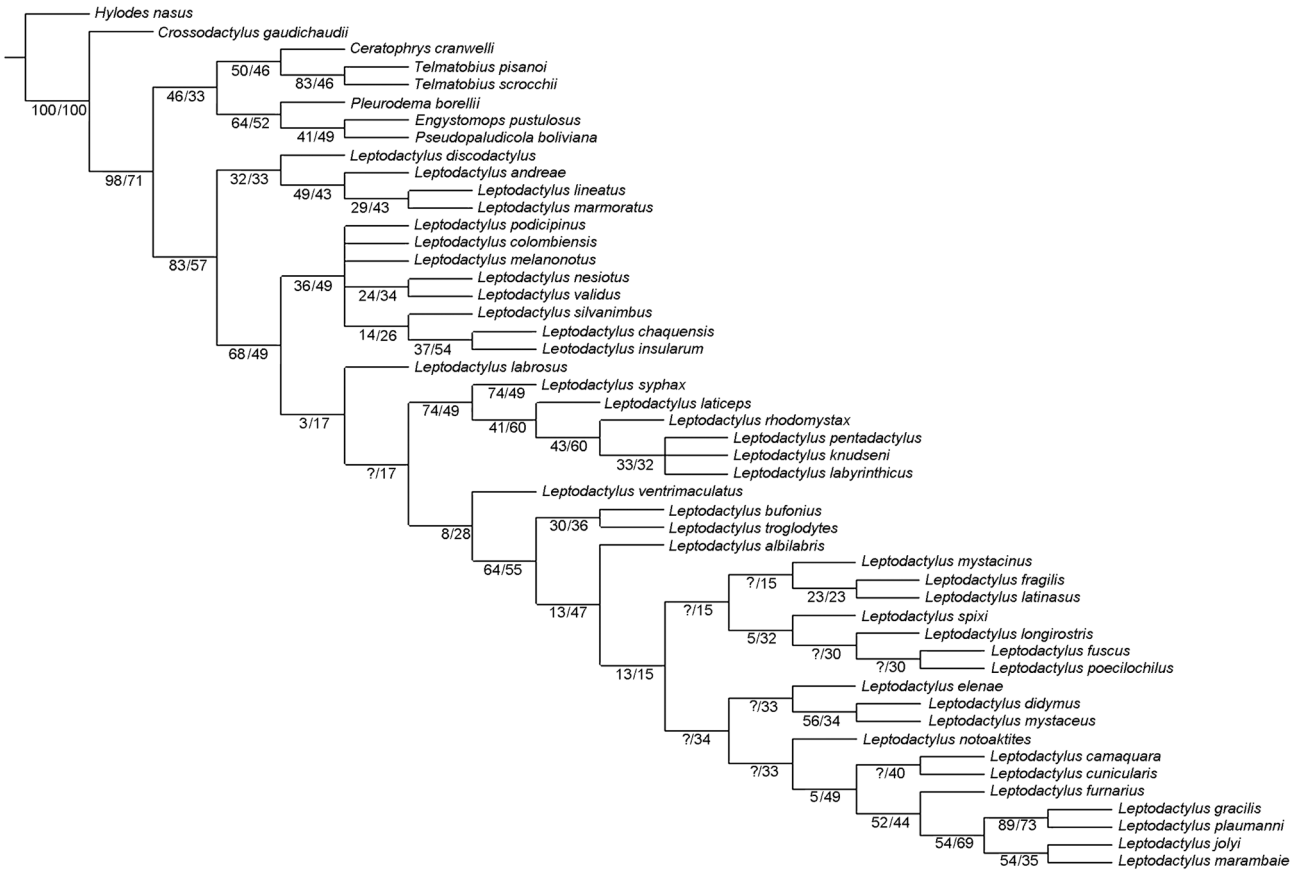

FIGURE 10. Topology of most parsimonious trees and bootstrap/GC/bremer support relative values under concavities K = 3. Question marks in GC values represent negatives values, which are an artifact of the method, assigned to weakly supported nodes.

Pelvic girdle (Fig. 8). The internal margins of the ilia form a U-shaped structure. A distinct dorsal prominence is located at the base of the ilial shaft above and anterior to the acetabulum. A very well-developed dorsal crest extends along the ilial shaft; the crest is almost uniform in width except anteriorly where diminishes in amplitude. The ilial shaft contacts with the sacral diapophyses sacral. The ilial shaft is round in cross section and the preacetabular angle is acute. The ilia are firmly fused with one another medially and with the ischia posteriorly. The pelvic plate is semicircular, and the acetabulum width is about twice its height. The posterior half of the acetabulum is formed by the ischium, which bears a supra-acetabular expansion that is about half the height of the ischium and as wide as the postacetabular portion of the bone. The acetabular portions of the ilium and ischium are almost equal in size. The dorsal edge of the ischium is above the level of the ilium. The pubis is localized as a wedge between the ilium and ischium.

Hind limb and pes (Fig. 9). The femur is weakly sigmoid. The tibiofibula is longer than the femur. A distinct *sulcus intermedius* marks the medial union of the tibia and fibula on both sides of the bone. A rounded

and cartilaginous sesamoid element is present at the tibiofibular-tibiale/fibulare joint, the cartilage sesamoides. The tibiale and fibulare are about half of the length of the tibiofibula, widely separated at their midpoint, and fused at their proximal and distal heads; they lack crests or flanges.

Three tarsal elements are present: element Y, Distal Tarsal 1, and Distal Tarsal 2–3. The element Y articulates with the base of the prehallux, Distal Tarsal 1, Tibiale, and Metatarsal I. Distal Tarsal 1 is the smallest and articulates with element Y, Distal Tarsal 2–3, tibiale, and Metatarsal I and II. Distal Tarsal 2–3 articulates mainly with Metatarsal III, but also with Metatarsal II and IV, and with Distal Tarsal 1, Tibiale, and Fibulare. There are 2 small plantar sesamoids below the tarsals, on the lateral side; the more lateral sesamoid is smaller than the more medial. The comparative lengths of the digits are IV > III > V > II > I. The digital phalangeal formula is: 2–2–3–4–3. The terminal phalanges end in divided tips. The prehallux consists of four segments.

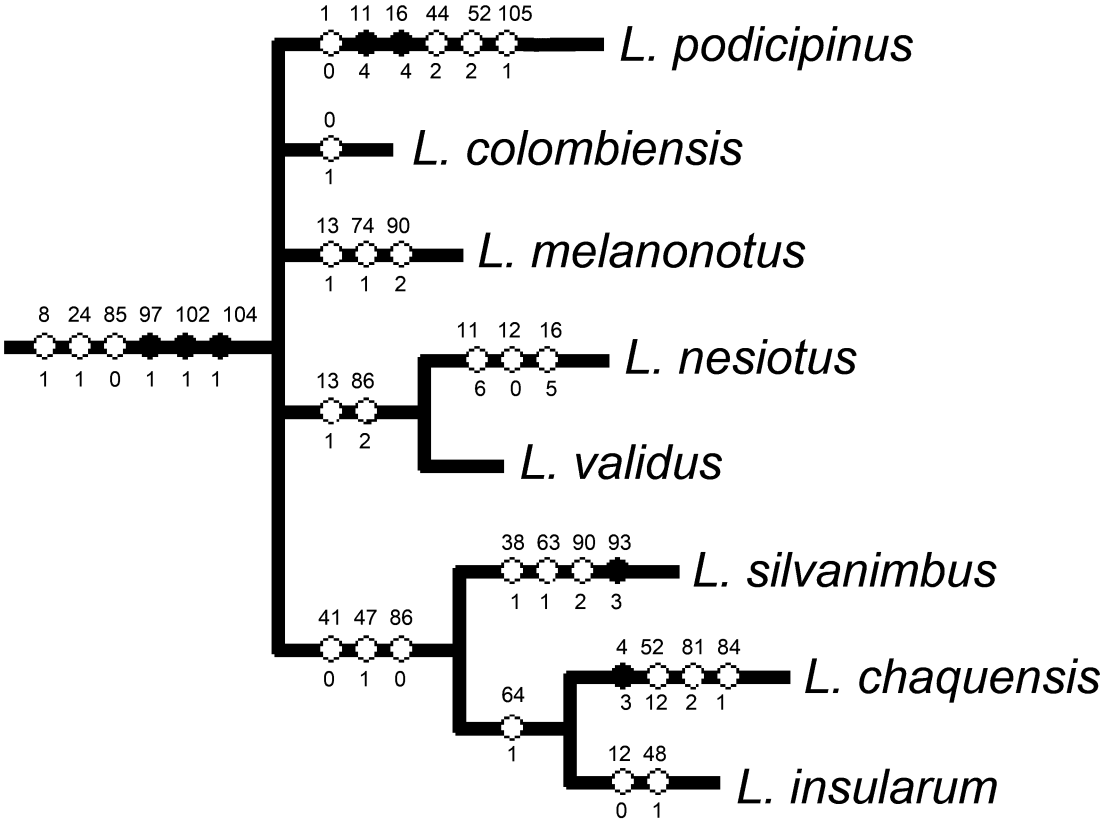

FIGURE 11. "*latrans-melanonotus*" clade with the synapomorphies for each node. Numbers above nodes are character numbers. Numbers below nodes are character states. Empty and filled hashmarks indicate homoplastic and non-homoplastic characters, respectively.

Phylogenetic relationships

The phylogenetic analysis resulted in ten most parsimonious trees (461 steps and fit = 76.94); the consensus tree is provided in Figure 10. *Leptodactylus nesiotus* is nested within a "*latrans-melanonotus*" clade (Fig. 11). This clade is supported by three synapomorphies in two of the cladograms obtained: dorsum with white tubercles posteriorly (Character 8:1, Fig. 12A), thumb with two lateral nuptial spines (Character 24:1 Fig. 12B), and *crista humeralis* in males (Character 85:0, Fig. 13A). Two additional synapomorphies support the *latrans-melanonotus* clade in other seven cladograms: *pars articularis quadrati* indistinct from *processus muscularis* (Character 97:1); larval *processus branchialis* closed (Character 102:1). In the remaining cladogram, the five synapomorphies previously mentioned defined the *latrans-melanonotus* group, plus the hyoquadrate process large and rounded (Character 104:1). *L. nesiotus* results as sister species to *L. validus*. This relationship is supported by two synapomorphies in three of the recovered cladograms: terminal

phalanges T-shaped (Character 86:2, Fig. 13 B) and dark-colored stripe on the outer side of arm present (Character 13:1 Fig. 12 B). Whereas, in the other seven cladograms, only the "terminal phalanges T-shaped" character supports their sister taxa relationship.

TABLE 1. Characters states and species added to the previously elaborated matrix of Ponssa (2008), and analyzed for this study.

	0	1	2	3	4	5	6	7	8	9	10	11	12	13	14	15	16	17	18
L.colombiensis	1	1	[01]	0	[01]	1	[01]	0	[12]	2	1	[16]	1	0	0	0	[15]	[01]	0
L.laticeps	0	0	0	0	0	0	[01]	0	0	0	1	6	1	0	0	0	5	0	0
L.nesiotus	0	1	[01]	0	1	1	1	0	[12]	2	1	6	0	1	1	0	5	1	0
L.melanonotus	0	1	0	0	0	1	[01]	0	[12]	2	1	[16]	[01]	10	[01]	1	[01]	0	1
L.silvanimbus	0	1	0	0	[01]	1	1	0	[12]	2	1	-	1	[01]	0	0	1	[01]	0
L.validus	0	1	[01]	0	[01]	1	1	0	1	2	1	1	1	1	[01]	0	1	[01]	0

continued.

	19	20	21	22	23	24	25	26	27	28	29	30	31	32	33	34	35	36
L.colombiensis	1	-	0	0	0	1	2	1	1	1	1	1	0	0	1	-	0	0
L.laticeps	1	1	0	0	0	1	2	1	1	1	1	1	0	0	0	-	0	0
L.nesiotus	1	-	0	-	0	1	2	1	1	1	1	1	0	0	1	-	0	0
L.melanonotus	-	0	0	0	1	2	1	1	1	1	1	0	0	1	-	0	0	[01]
L.silvanimbus	1	-	0	0	0	1	2	1	1	1	1	1	0	0	1	-	0	0
L.validus	1	-	0	0	0	1	2	1	1	1	1	1	0	0	1	-	0	0

continued.

	37	38	39	40	41	42	43	44	45	46	47	48	49	50	51	52
L.colombiensis	1	[01]	0	1	1	0	0	1	0	1	-	[12]	0	0	0	[01]
L.laticeps	1	[01]	0	1	0	0	0	[12]	0	1	1	[12]	2	0	0	2
L.nesiotus	1	0	0	1	1	0	0	1	0	1	0	[12]	0	0	0	0
L.melanonotus	[01]	0	1	1	0	0	[12]	0	1	0	[012]	0	0	0	[012]	1
L.silvanimbus	1	1	0	1	0	0	0	1	0	1	1	2	0	0	0	0
L.validus	1	[01]	0	1	10	0	[12]	0	1	0	2	0	0	0	[01]	1

continued.

	53	54	55	56	57	58	59	60	61	62	63	64	65	66	67	68	69
L.colombiensis	1	1	[01]	0	-	[01]	1	1	[01]	1	[12]	0	[01]	1	0	-	2
L.laticeps	0	1	1	0	-	0	1	1	1	1	3	0	1	1	0	-	[12]
L.nesiotus	1	1	0	0	-	1	1	1	1	1	[1,2]	0	1	1	0	-	2
L.melanonotus	1	0	0	-	[01]	1	1	1	1	1	2	0	1	0	0	2	2
L.silvanimbus	1	1	0	0	-	1	1	1	1	1	1	0	1	1	0	-	2
L.validus	1	[01]	0	-	[01]	1	1	1	1	2	2	0	1	0	0	2	2

continued.

	70	71	72	73	74	75	76	77	78	79	80	81	82	83	84	85	86
L.colombiensis	0	0	0	[01]	0	0	0	0	2	0	0	-	0	[12]	0	0	[01]
L.laticeps	0	0	0	0	0	0	0	0	2	0	0	-	0	0	1	0	[01]
L.melanonotus	0	0	0	1	0	0	0	0	2	0	0	[01]	0	[12]	0	0	[01]
L.nesiotus	0	0	0	1	0	0	0	0	2	0	0	1	0	1	0	0	2
L.silvanimbus	0	0	-	-	-	-	-	0	2	-	-	-	-	-	-	0	0
L.validus	0	0	0	[01]	0	0	0	0	2	0	0	0	0	1	0	0	2

continued.

	87	88	89	90	91	92	93	94	95	96	97	98	99	100	101	102	103	104
L.colombiensis	1	1	-	-	-	-	-	-	-	-	-	-	-	-	-	-	-	-
L.laticeps	1	1	-	-	-	-	-	-	-	-	-	-	-	-	-	-	-	-
L.melanonotus	1	1	-	2	0	0	[03]	-	0	0	1	0	1	-	0	1	-	-
L.nesiotus	1	1	-	-	-	-	-	-	-	-	-	-	-	-	-	-	-	-
L.silvanimbus	1	1	-	2	1	0	3	-	0	0	1	0	1	-	0	1	-	-
L.validus	1	1	-	-	-	-	-	-	-	-	-	-	-	-	-	-	-	-

Discussion

Our analyses do not recover a monophyletic *L. melanonotus* group. Instead, our results support previous studies that suggest that the *L. melanonotus* species group is paraphyletic to the *L. latrans* group (Heyer 1998, Larson & de Sá 1998). Larson and de Sá (1998) identified a monophyletic "*latrans-melanonotus*" clade supported by five chondrocranial characters: 1) narrow *suprarostral corpora*, widely separated and not attached distally to the alae, 2) narrow and widely divergent *cornua trabeculae*, 3) *pars articularis quadrati* indistinct from the *processus muscularis* in lateral view, 4) presence of a closed *processus branchialis*, and 5) a narrow *planum trabeculare anticum* posterior to the confluence of the *cornua trabeculae*. Although, Ponssa (2008) included only three species of each of the *melanonotus* and *latrans* species groups, the last three chondrocranial characters listed above also supported a *latrans-melanonotus* clade. Furthermore, two additional characters supported this clade: 1) posterolateral extension of the palatoquadrate reaches a third of the length of the otic capsule and 2) hyoquadrate process large and rounded in lateral view. Previously, Lynch (1971) suggested that the "…*melanonotus* group is a composite with part of the species (those with arched prevomerine dentigerous processes of the prevomerine bones) being members of the *latrans* group". Although our taxon sampling is limited, the results agree with Larson and de Sá's (1998) suggestion that the *melanonotus* and *latrans* groups together form a monophyletic clade. *L. nesiotus* resulted phylogenetically closer to *L. validus*, a relationship supported by two synapomorphies (see results). The character "terminal phalanges T-shaped" is also found among several other species, including *L. diedrus* (Heyer, 1998), in species of the subgenus *Lithodytes* (Heyer 1974; 1998; Ponssa & Heyer 2007), in *L. silvanimbus* and *L. leptodactyloides* (Heyer 1998), and in some species of the *L. fuscus* group (Ponssa 2008). In *L. laticeps* the terminal phalanges are knobbed or rounded and bifurcated (Ponssa 2006). Although *L. validus* has a more extensive distribution that includes northern South America (Camargo *et al*. 2006), the species overlap in Trinidad (with *L. nesiotus* being endemic to this island). The two species are easily differentiated based on external morphology: *L. nesiotus* has a broad light stripe on the entire upper lip or at least extending under the eye, stripe lacking in *L. validus* (Heyer 1994). The skeletal morphology is almost identical in both species; the slight differences found are in characters that exhibit some level of polymorphism. The osteological differences between the two species are (*L. validus* characters provided in parentheses): 1) *pars facialis* of maxilla do not contact the nasal in *L. nesiotus* (*pars facialis* of maxilla may or may not contact the nasal), 2) sphenethmoid extends only half the length of the nasals (sphenethmoid may extend to the posterior end of the nasals), 3) nasal do not contact each other (nasals may contact medially or anteriorly), 4) the postero-medial angle of nasals does not contact the frontoparietals (occasionally adjacent or in contact with frontoparietals), 5) cultriform process of parasphenoid does not reach the neopalatines (process may extend between the neopalatines), 6) anteromedial process of hyoid present (anteromedial process of hyoid either present or absent).

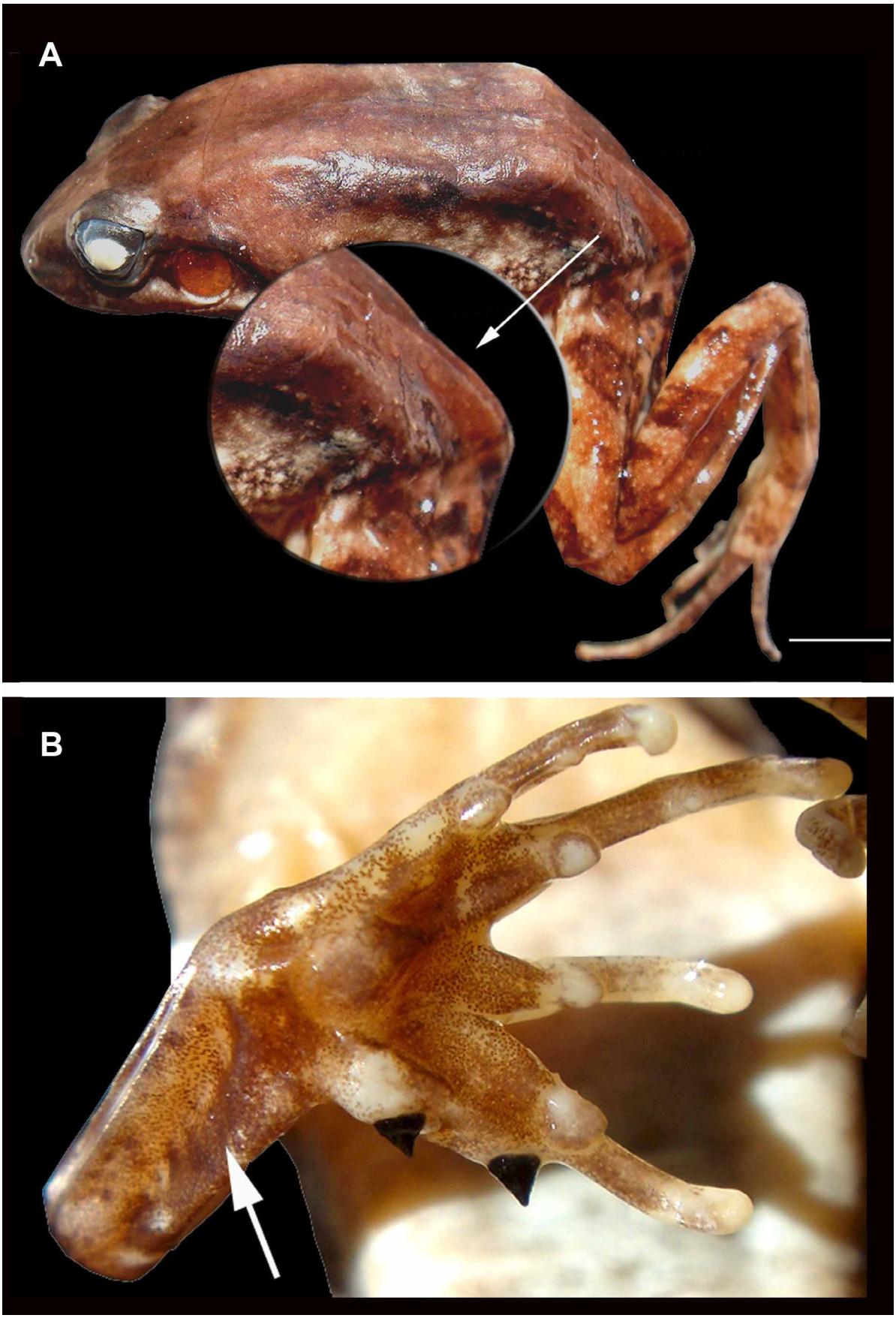

FIGURE 12. Male of *Leptodactylus nesiotus* showing: (A) Dorsum with white tubercles posteriorly; (B) Dark-colored stripe on the outer side of arm and thumb with two lateral nuptial spines. Scale bar = 5 mm.

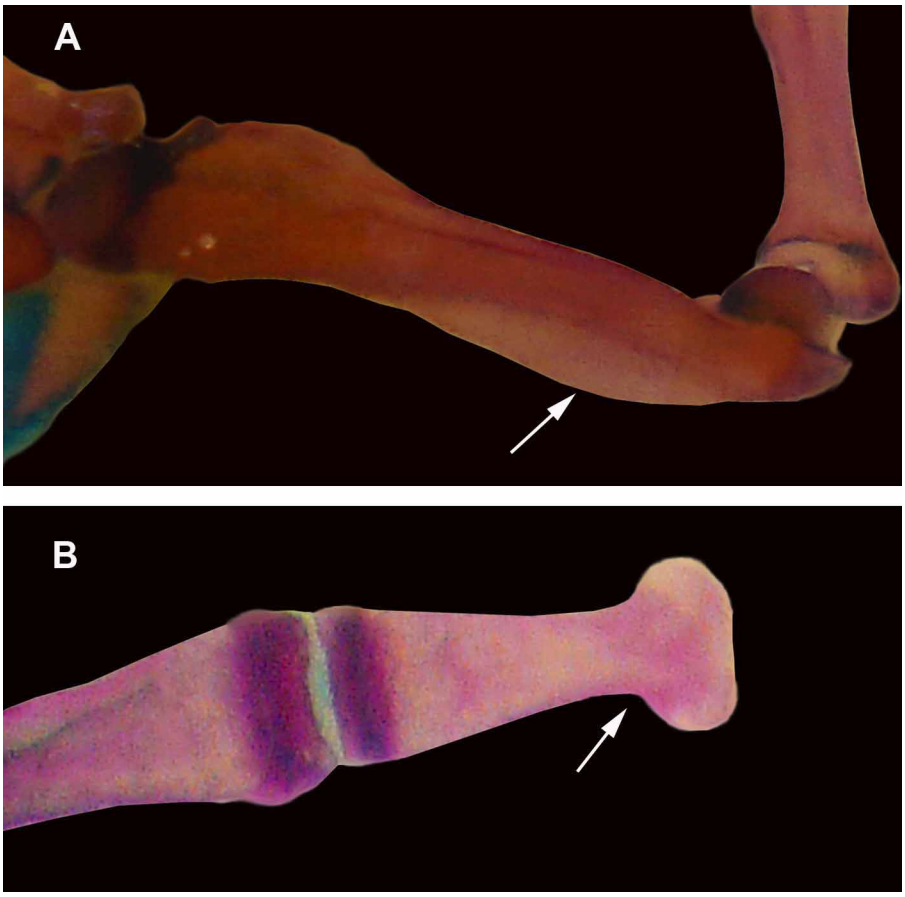

FIGURE 13. (A) *Crista humeralis* in male of *Leptodactylus nesiotus*. (B) T-shaped terminal phalange of the finger IV.

The skeleton of *Leptodactylus nesiotus* was compared with available descriptions for species of other *Leptodactylus* groups: *L. leptodactyloides*, *L. melanonotus*, *L. diedrus*, *L. discodactylus*, *L. riveroi*, and *L. silvanimbus* (Heyer 1998), *L. insularum* (Heyer 1998; Ponssa 2008), *L. chaquensis* (Heyer 1998; Perotti 2001; Ponssa 2008), *L. laticeps* (Ponssa 2006), *L. pentadactylus* (Heyer 1969b; 1998), *L. lauramiriamae* (Heyer & Crombie 2005), species of the *L. fuscus* group (Heyer 1998; Ponssa & Lavilla 1998; Ponssa 2008; Sebenn *et al*. 2007), and species of the subgenus *Lithodytes* (Heyer 1974; 1998; Ponssa & Heyer 2007). The main differences found are listed in Table 2.

Leptodactylus nesiotus skeletal morphology reveals useful taxonomical characters for comparative analyses within the genus. This data is useful to assess in a comparative manner the evolutionary relationships, the morphological variation, and the evolution of shape changes in *Leptodactylus*. Consequently, the comparison of anatomical characters is of fundamental importance to achieve an approximation to a total evidence approach which includes molecular data among others.

Acknowledgements

We wish to thank the Trinidad and the Wildlife Section of the Trinidadian Government for permission to do the work. Many Glasgow University students helped in this project, in particular Roisin Campbell-Palmer. This study was supported by National Science Foundation, USA, award 0342918 to RdS and WRH. MJJ fieldwork was supported by a UK Natural Environmental Research Council postgraduate studentship. MLP thanks CONICET (PIP 112-200801-00225) and FONCyT (PICT Nº12418-06-223 and Nº 2008-0578), Argentina, and NSF award 0342918 to RdS and WRH.

TABLE 2. Osteological characters differences between *Leptodactylus nesiotus* and other species of the genus. In parenthesis are the corresponding numbers of the characters used in the analysis of the present study.

Character	*L. nesiotus*	other *Leptodactylus*	References
Pseudodontoid (character 31)	absent	present in *L. troglodytes.*	Sebben *et al*. 2007; Ponssa 2008
Alary process of premaxilla (character 33)	dorsally directed	posterodorsally directed in *L. laticeps*, *L. chaquensis*, *L. insularum.*	Ponssa 2006; 2008
Pars facialis of maxilla (character 38)	separated of the nasals	contiguous with nasals in *L. ventrimaculatus*, and in some specimens of *L. bufonius*, *L. labrosus*, *L. laticeps* and *L. troglodytes*.	Ponssa 2006; 2008
Prenasal process of the *tectum nasi* (character 42)	absent	present in the most of the species of the *L. fuscus* groups, such as *L. bufonius*, *L. camaquara*, *L. cunicularis*, *L. didymus*, *L. furnarius*, *L. fuscus*, *L. gracilis*, *L. jolyi*, *L. fragilis*, *L. longirostris*, *L. marambaie*, *L. mystaceus*, *L. plaumanni*, *L. poecilochilus*, *L. troglodytes*, *L.ventrimaculatus* and some specimens of *L. mystacinus*.	Ponssa 2008
Tectum nasi (character 41)	at the same level of the alary processes of premaxillae	posterior to the alary processes in *L. laticeps*, *L. chaquensis*, *L. insularum*, *L. notoaktites* and in some specimens of *L. marmoratus*, *L. albilabris*, *L. latinasus*, *L. mystacinus*, *L. plaumanni*, *L. spixi* and *L. labrosus*; it is anterior to the alary processes in *L. bufonius*, *L. camaquara*, *L. cunicularis*, *L. troglodytes*, and in some specimens of *L. fuscus*, *L. furnarius*, *L. gracilis*, *L. fragilis*, *L. longirostris* and *L. poecilochilus*.	Ponssa 2008
Sphenethmoid	does not reach the optic foramina	it is contacting joins to the optic foramina in *L. pentadactylus*, *L. bufonius*, *L. fuscus* and in some specimens of *L. laticeps*, *L. marmoratus* and *L. lineatus*.	Heyer 1969b; 1998; Ponssa 2006
Posterolateral prolongations of frontoparietals (character 47)	short	longer in *L. laticeps*, *L. pentadactylus*, *L. chaquensis* and *L. riveroi*.	Heyer 1998; Ponssa 2006; 2008
Anterior portion of the frontoparietals	approximately of uniform width	gradually expands towards the anterior plane in *L. laticeps.*	Ponssa 2006
Nasals (character 52)	separated	adjacent or in contact to each other in the middle or anterior zone of the medial borders in *L. fragilis*, *L. troglodytes*, in some specimens of *L. melanonotus*, *L. leptodactyloides*, *L. marmoratus*, *L. andreae*, *L. chaquensis*, *L. albilabris*, *L. fuscus*, *L. gracilis*, *L. latinasus* and *L. spixi*; they are adjacent or in contact to each other along its medial borders in *L. laticeps*, *L. labrosus*, *L. mystacinus*, *L. ventrimaculatus*, in some specimens of *L. podicipinus*, *L. chaquensis*, *L. bufonius*, *L. fuscus*, *L. melanonotus* and *L. leptodactyloides*.	Heyer 1974; Ponssa & Lavilla 1998; Perotti 2001; Ponssa 1998; 2008)
Maxillary process of nasals (character 54)	well differentiated from the nasal body	weakly differentiated from the nasal body in *L. bufonius*, *L. gracilis*, *L. fragilis*, *L. latinasus*, *L. mystacinus*, *L. plaumanni*, and in some specimens of *L. andreae*, *L. mystaceus* and *L. troglodytes*.	Ponssa & Lavilla 1998; Ponssa 2008
Postero-medial angle of nasals (character 55)	separated from the frontoparietals	adjacent or in contacts with frontoparietals in *L. laticeps*, *L. discoidalis*, *L. labrosus*, in some specimens of *L. podicipinus*, *L. chaquensis*, *L. mystacinus* and in *L. ventrimaculatus*.	Perotti 2001; Ponssa 2006; 2008

continued next page

TABLE 2. (continued)

Character	*L. nesiotus*	other *Leptodactylus.*	References
Cultriform process of parasphenoid (character 58)	does not reach the neopalatines	extends at the level of the neopalatines in *L. silvanimbus*, *L. laticeps*, the species of the *L. fuscus* group, some specimens of *L. podicipinus*, *L. melanonotus*, *L. insularum*, *L. lineatus* and in *L. chaquensis*.	Ponssa 2006; 2008
Vomerine teeth (character 61)	in an arched series	outline a straight row in *L. podicipinus*, *L. lauramiriamae*, *L. discodactylus*, in some specimens of *L. melanonotus*, *L. marmoratus*, *L. cunicularis*, *L. furnarius*, *L. gracilis*, *L. fragilis*, *L. latinasus*, *L. plaumanni*, *L. andreae* and in *L. lineatus*.	Heyer & Crombie 2005; Ponssa 2008
Dentigerous processes of vomers (character 62)	horizontal	is inclined or diagonal in *L. lineatus*, in some specimens of *L. marmoratus*, *L. andreae* and in *L. discodactylus*.	Ponssa & Heyer 2007; Ponssa 2008
Anterior ramus of vomer	contacts the maxilla or the premaxilla	does not reach the maxilla or the premaxilla in *L. silvanimbus*, *L. laticeps*, *L. chaquensis*, in some specimens of *L. podicipinus*, *L. melanonotus*, *L. insularum*, *L. lineatus*, *L. fuscus*.	Heyer 1974; 1998;
Palatine	with a superficial and hardly noticeable ridge	with a prominent and serrated ridge in *L. laticeps*.	Ponssa 2006
Palatines	arched	practically straight in some specimens of *L. laticeps*	Ponssa 2006
Pterygoid and parasphenoid	overlap in the antero-posterior plane	do not overlap in some specimens of *L. melanonotus.*	Heyer 1998
Otic ramus of squamosal (character 69)	overlaps the crista parotica	just reaches the border of the crista parotica in *L. camaquara*, *L. cunicularis*, *L. didymus*, *L. fuscus*, *L. jolyi*, *L. fragilis*, *L. furnarius*, *L. marambaie*, *L. mystaceus*, in some specimens of *L. podicipinus*, *L. laticeps*, *L. marmoratus*, *L. bufonius*, *L. mystacinus*, *L. notoaktites*, *L. poecilochilus* and *L. troglodytes*; or it does not contact the crista parotica in *L. elenae*, *L. gracilis*, *L. latinasus* and in some specimens of *L. bufonius.*	Ponssa 2008
Alary process of hyoid (character 72)	narrow base, stalk-like	broad based in *L. marmoratus*, *L. andreae* and *L. lineatus*.	Heyer 1998; Ponssa 2008
Hyoid plate	slightly wider than long	notoriously wider than longer in *L. laticeps*; it is longer than wider in *L. marmoratus* and *L. andreae*	Ponssa 2006; Ponssa & Heyer 2007
cotylar arrangement (according to Lynch, 1971)	type I	type II in *L. laticeps*.	Ponssa 2006
Bases of the occipital condyles	posterior to the most posterior points of either the squamosals or maxillae	are anterior to this points in *L. laticeps*.	Ponssa 2006
Carpal elements	five (Fabrezi's, 1992 type E)	six (Fabrezi's, 1992 type C) in *L. laticeps*, *L. andreae*, *L. marmoratus* and while *L. lineatus*	Ponssa 2006; Ponssa & Heyer 2007
Crista humeral in males (character 85)	on the distal half to two-thirds of the humerus	present along the length of humerus in *L. laticeps*; it is absent in the species of the *L. fuscus* group, *L. marmoratus*, *L. andreae*, *L. lineatus* and *L. discodactylus*.	Ponssa 2006; Ponssa & Heyer 2007; Ponssa 2008

References

Camargo, A., de Sá, R.O. & Heyer, W.R. (2006) Phylogenetic analyses of mtDNA sequences reveal three cryptic lineages in the widespread neotropical frog *Leptodactylus fuscus* (Schneider, 1799) (Anura, Leptodactylidae). *Biological Journal of the Linnean Society*, 87, 325–341.

de Sá, R.O., Heyer, W.R. & Camargo, A. (2005) Are *Leptodactylus didymus* and *L. mystaceus* phylogenetically sibling species (Amphibia, Anura, Leptodactylidae)? *Herpetologia Petropolitana*, 90–92.

Fabrezi, M. (1992) El carpo de anuros. *Alytes*, 10, 1–36.

Fabrezi, M. & Alberch, P. (1996) The carpal elements of anurans. *Herpetologica*, 52, 188–204.

Farris, J.S. (1969) A successive approximations approach to character weighting. *Systematic Zoology*, 18, 374–385.

Farris, J.S. (1988) Hennig86, program and documentation. Published by the author, Port Jefferson, New York.

Fitzinger, L.J.F.J. (1826) Neue Classification der Reptilien nach ihren natu¨rlichen Verwandtschaften nebst einer Verwandtschafts-Tafel und einem Verzeichnisse der Reptilien-Sammlung des k.k. zoologisch Museum's zu Wien. Wien: J.G. Heubner.

Frost, D.R. (2009) Amphibian Species of the World: an Online Reference. Version 5.2 (15 July, 2008). Electronic Database available from: http://research.amnh.org/ herpetology/amphibia/index.php. American Museum of Natural History, New York, USA (accessed March 2 2010).

Goloboff, P.A. (1993) Estimating character weigths during tree search. *Cladistics*, 9, 83–91.

Goloboff, P.A. (1997) Self-weighted optimization: tree searches and character states reconstruction under implied transformation costs. *Cladistics*, 13, 225–245.

Goloboff, P.A. & Farris, J.S. (2001) Methods for quick consensus estimation. *Cladistics*, 17, 26–34.

Goloboff, P., Farris, J. & Nixon, K. (2003a) T.N.T.: tree analysis using new technology. Program and documentation available from the authors and http://www.zmuc.dk/public/ phylogeny (accessed March 2 2010).

Goloboff, P.A., Farris, J.S., Källersjö, M., Oxelman, B., Ramírez, M.J. & Szumik, C.A. (2003b) Improvements to resampling measures of group support. *Cladistics*, 19, 324–332.

Heyer, W.R. (1969a) The adaptive ecology of the species groups o the genus *Leptodactylus* (Amphibia, Leptodactylidae). *Evolution*, 23, 421–428.

Heyer, W.R. (1969b) Studies on the genus *Leptodactylus* (Amphibia, Leptodactylidae) III. A redefinition of the genus *Leptodactylus* and a description of a new genus of Leptodactylid frogs. *Contribution in Science, Natural History Museum Los Angeles County*, 155, 1–14.

Heyer, W.R. (1974) Relationships of the *marmoratus* species group (Amphibia, Leptodactylidae) within the subfamily Leptodactylinae. *Contributions in Science of the Natural History Museum of the Los Angeles County*, 253, 1–46.

Heyer, W.R. (1994) Variation within then *Leptodactylus podicipinus-wagneri* complex of frogs (Amphibia: Leptodactylidae). *Smithsonian Contributions to Zoology*, 546, 1–124.

Heyer, W.R. (1998) The relationships of *Leptodactylus diedrus* (Anura, Leptodactylidae). *Alytes*, 16, 1–24.

Heyer, W.R. & Crombie, R.I. (2005) *Leptodactylus lauramiriamae*, a distinctive new species of frog (Amphibia: Anura: Leptodactylidae) from Rondônia, Brazil. *Preceedings of the Biological Society of Washington*, 118, 590–595.

IUCN, Conservation International, and Nature Serve. (2006) Global Amphibian Assessment. www.globalamphibians.org. (accessed 12 November 2008)

Larson, P.M. & de Sá, R.O. (1998) Chondrocranial morphology of *Leptodactylus* larvae (Leptodactylidae: Leptodactylinae): its utility in phylogenetic reconstruction. *Journal of Morphology*, 238, 287–305.

Lavilla, E.O., Langone, J.A., Caramaschi, U., Heyer, W.R. & de Sá, R.O. (2010) The identification of *Rana ocellata* Linnaeus, 1758. Nomenclatrual impact on the species currently known as *Leptodactylus ocellatus* (Leptodactylidae) and *Osteopilus brunneus* (Gosse, 1851) (Hylidae). *Zootaxa*, 2346, 1–16.

Lipscomb, D.L. (1992) Parsimony, homology and the analysis of multistate characters. *Cladistics*, 8, 45–65.

Lynch, J.D. (1971) Evolutionary relationships, osteology, and zoogeography of leptodactyloid frogs. *Miscellaneous Publications Museum of Natural History University of Kansas*, 53, 1–238.

Maglia, A.M., Pugener, L.A. & Mueller, J.M. (2007) Skeletal morphology and postmetamorphic ontogeny of *Acris crepitans* (Anura: Hylidae): a case of miniaturization in frogs. *Journal of Morphology*, 268, 194–223.

Maxson, L.R. & Heyer, W.R. (1988) Molecular systematics of the frogs genus *Leptodactylus* (Amphibia: Leptodactylidae). *Fieldana: Zoology*, 41, 1–13.

Perotti, M.G. (2001) Skeletal development of *Leptodactylus chaquensis* (Anura: Leptodactylidae). *Herpetologica*, 57, 318–335.

Ponssa, M.L. (2006) On the osteology of a distinctive species of the genus *Leptodactylus*: *Leptodactylus laticeps* (Boulenger, 1917) (Anura, Leptodactylidae). *Zootaxa*, 1188, 23–36.

Ponssa, M.L. (2008) Cladistic analysis and osteological descriptions of the species of the *L. fuscus* species group of the genus *Leptodactylus* (Anura, Leptodactylidae). *Journal of Zoological Systematics and Evolutionary Research*, 46, 249–266.

Ponssa, M.L., Goldberg, J. & Abdala, V. (2010) Sesamoids in anurans: new data, old issues. *Anatomical Record*, 293, 1646–1668.
Ponssa, M.L. & Heyer, W.R. (2007) Osteological characterization of four putative species of the genus *Adenomera* (Anura: Leptodactylidae), with comments on intra- and interspecific variation. *Zootaxa*, 1403, 37–54.
Ponssa, M.L. & Lavilla, E.O. (1998) Osteology of *Leptodactylus latinasus* (Anura: Leptodactylidae) and the validity of its subspecies. *Bulletin of the Maryland Herpetological Society*, 34, 57–63.
Pugener, L.A. & Maglia, A.M. (2007) Skeletal morphology and development of the olfactory region of *Spea* (Anura: Scaphiopodidae). *Journal of Anatomy*, 211, 754–768.
Sebben, A., Maciel, N.M., Campos, L.A., Kokubum, M.N.C. & Da Silva, H.R. (2007) Occurrence of a calcified pseudodontoid in *Leptodactylus troglodytes* (Anura: Leptodactylidae). *Journal of Herpetology*, 41, 337–340.
Trewavas, E. (1933) The hyoid and larynx of the Anura. *Philosophical Transactions of the Royal Society of London*, 222, 401–527.
Trueb, L. (1973) Bones, frogs and evolution. *In*: Vial, J. L. (Ed.), *Evolutionary biology of the anurans: contemporary research on major problems*. The University Missouri Press, Columbia, pp. 65–132.
Trueb, L. (1993) Patterns of cranial diversity among the Lissamphibia. *In*: Hanken, J. & B. K. Hall (Eds.), *The Skull 2*. The University of Chicago Press, pp. 255–343.
Trueb, L., Pugener, L.A. & Maglia, A.M. (2000) Ontogeny of the bizarre: an osteological description of *Pipa pipa* (Anura: Pipidae), with an account of skeletal development in the species. *Journal of Morphology*, 243, 75–104.
Wassersug, R.J. (1976) A procedure for differential staining of cartilage and bone in hole formalin fixed vertebrates. *Staining Technology*, 51, 131–134.

Appendix 1. Characters used in the parsimony analysis, after Ponssa (2008).

0. Longitudinal mid-dorsal stripe. (0) absent; (1) present, from the vent to the space between or behind the eyes; (2) present, from the vent to the tip of the snout. It is present as a light-coloured stripe.
1. Lateral cephalic stripe. (0) distinct; (1) indistinct.
2. Light-coloured stripe in the posterior surfaces of the thigh. (0) indistinct; (1) distinct.
3. Longitudinal light-coloured lines on the dorsal surface of the tibia. (0) absent; (1) present.
4. Dorsolateral folds. (0) absent; (1) 2–4; (2) 6; (3) 8.
5. Tibia-tarsal texture. (0) smooth; (1) with tubercles.
6. Texture of foot surface. (0) smooth; (1) with tubercles.
7. Mid-dorsal light-coloured line from the vent to the tip of the snout. (0) absent; (1) present.
8. Dorsum. (0) without white tubercles; (1) white tubercles posteriorly; (2) white tubercles on all dorsal surfaces. This character was treated as additive.
9. Toe webbing. (0) no web or fringe; (1) weak basal fringes and/or webbing; (2) toes with fringes extending on both sides of toes, not on tips; (3) toes webbed. This character was treated as additive.
10. Dark stripe on the upper lip. (0) well defined; (1) not well defined or absent.
11. Venter. (0) immaculate; (1) with spots laterally; (2) completely pigmented; (3) gray or similar with white spots; (4) brown with white rounded areas without spots; (5) anteriorly dark with a middle light line, posteriorly with dark irregular spots; (6) light with dark spots, vermiculations or labyrinthine.
12. Dark-coloured canthal and supratympanic stripe from nostril to shoulder. (0) present; (1) absent.
13. Dark-coloured stripe on the outer side of arm. (0) absent; (1) present.
14. Light-coloured spot in the center of dorsum. (0) absent; (1) present.
15. Postympanic gland. (0) not pigmented; (1) pigmented in males.
16. Ventral surfaces of thighs. (0) immaculate; (1) with spots on borders; (2) completely coloured; (3) gray or similar with white spots; (4) with black spots and rounded areas without spots; (5) light with dark vermiculations, spots or labyrinthine.
17. White tubercles on head and arms. (0) absent; (1) present.
18. Toe tips. (0) not expanded; (1) with an undivided expansion; (2) expanded with a middle dorsal sulcus that separates two protuberances.
19. Fold on the inner side of tarsus. (0) present; (1) absent.
20. Fingers. (0) with fringes; (1) without fringes.
21. Mid-tarsal tubercle. (0) absent; (1) present.
22. Light interscapular spot. (0) absent; (1) present.
23. Coloration of arms. (0) one color; (1) bicolor.
24. Nuptial excrescences. (0) absent; (1) thumb with two lateral spines; (2) thumb with three or more dorsal spines; (3) thumb with a couple of nuptial callosities, which are sandpaper-like patches of skin; (4) thumb with many small spines; (5) thumb with one lateral spine.

25. Snout in lateral view. (0) protruding; (1) truncate; (2) round; (3) sloping.
26. Pectoral glands. (0) present; (1) absent.
27. Fold or ridge extending the length of fore-arm. (0) present; (1) absent.
28. Upper eyelid. (0) triangular; (1) rounded.
29. Outer metatarsal tubercle. (0) spade-like; (1) long, of normal development.
30. Supratympanic fold. (0) indistinct; (1) distinct.
31. Hypertrophy of the mandibular symphysis (pseudodontoid). (0) absent; (1) present.
32. Odontoids of dentary. (0) absent; (1) present.
33. Alary processes of premaxillae. (0) posterodorsally directed; (1) dorsally directed; (2) anterodorsally directed.
34. Alary processes of premaxillae. (0) distal half of alary process of premaxillae aligned with the main axis of the process; (1) superior half of alary process of premaxillae slightly directed outwards and undivided, although the extremity can be divided; (2) superior half of alary process of premaxillae directed outwards at an angle of approximately 45º; it ends in two acute processes.
35. Base of alary processes of premaxillae. (0) sub-equal or narrower than the extreme; (1) broader than the extreme.
36. *Pars palatina* of premaxilla. (0) with a wide concavity; (1) with a narrow concavity.
37. *Pars facialis* of maxilla. (0) ends before level of neopalatines; (1) ends at level of neopalatines; (2) ends behind level of neopalatines. This character was treated as additive.
38. *Pars facialis* of maxilla. (0) separated from nasals; (1) contiguous to nasals.
39. *Pars facialis* of maxilla. (0) gradually decreases in height; (1) abruptly decreases its height.
40. Anterior extreme of maxilla. (0) straight; (1) with a lateral projection.
41. Position of *tectum nasi* relative to alary processes of premaxillae. (0) posterior; (1) at the same level; (2) anterior. This character was treated as additive.
42. Anterior projection of *tectum nasi*. (0) straight; (1) with a slightly developed projection; (2) with a well differentiated projection.
43. *Tectum nasi* and *solum nasi*. (0) cartilaginous; (1) mineralized.
44. Relationship between sphenethmoid and nasals in antero-posterior plane. (0) sphenethmoid and *septum nasi* fused. The relative position of nasals is indistinguishable; (1) sphenethmoid reaches half the length of the nasals; (2) sphenethmoid reaches the posterior extreme of the nasals; (3) nasals and sphenethmoid not overlapping; (4) sphenethmoid reaches the posterior 2/3 of the nasals.
45. Sphenethmoid. (0) dorsally visible; (1) not dorsally visible.
46. Frontoparietal fontanelle. (0) not completely covered by frontoparietals; (1) completely covered by frontoparietals.
47. Posterolateral processes of frontoparietals. (0) no projection or minimal, such as a swelling; (1) distinctive, relatively short processes.
48. Posterior margin of frontoparietals. (0) concave; (1) straight; (2) convex; (3) protuberant. This character was treated as additive.
49. Anterior portion of frontoparietals. (0) of uniform width; (1) gradually expanding towards posterior plane; (2) expanding toward the anterior plane.
50. Frontoparietals. (0) paired; (1) single, without space or suture that divide the frontoparietals in the posterior half.
51. Frontoparietals. (0) without a notch dividing the anterior region (frontals) from the posterior one (parietals); (1) with a notch dividing the anterior region from the posterior one.
52. Nasals. (0) broadly separated; (1) close to each other or in contact in the middle or anterior zone; (2) close to each other or in contact along its inner border.
53. Anterior border of nasals. (0) deeply concave; (1) slightly concave; (2) straight; (3) slightly convex or irregular. This character was treated as additive.
54. Maxillary process of nasals. (0) slightly differentiated from nasal body; (1) well differentiated from the nasal body.
55. Postero-internal angle of nasals. (0) broadly separated from frontoparietals; (1) close to each other or in contact with frontoparietals.
56. Shape of nasals. (0) triangular; (1) rhomboidal; (2) claw-shaped; (3) ovoid.
57. Anterior border of the nasals. (0) behind the level of the anterior extreme of maxillae; (1) at the level of the anterior extreme of maxillae; (2) before the anterior extreme of maxillae.
58. Extension of cultriform process of parasphenoid. (0) between neopalatines; (1) not reaching the neopalatines.
59. Cultriform process of parasphenoid. (0) with keel; (1) without keel.
60. Cultriform process of parasphenoid. (0) anteriorly expanded; (1) expanded in the middle area; (2) posteriorly expanded. This character was treated as additive.
61. Vomerine teeth. (0) in a straight line; (1) in an arched series.
62. Orientation of dentigerous processes of vomers. (0) diagonal; (1) horizontal.
63. Number of vomerine teeth**.** (0) none; (1) fewer than or equal to 7; (2) from 8 to 13; (3) equal to or more than 14.
64. Vomers. (0) separated; (1) contiguous or in contact.
65. Anterior ala of vomers. (0) broad; (1) acute; (2) absent.

66. Relationships between neopalatines and vomers. (0) not in contact; (1) vomers overlap neopalatines.
67. Pterygoid. (0) does not reach the neopalatines; (1) reaches the neopalatines.
68. Otic ramus of squamosal. (0) wider than zygomatic ramus; (1) as broad as zygomatic ramus; (2) narrower than zygomatic ramus.
69. Otic ramus of squamosal. (0) does not contact the *crista parotica*; (1) reaches the border of the crista parotica; (2) overlaps the crista parotica. It was treated as additive.
70. Anterior ramus of squamosal. (0) normal development; (1) vestigial.
71. Quadratojugal. (0) present; (1) absent.
72. Anterodorsal (alary) process of hyoid. (0) narrow, stalk-like; (1) broad based; (2) wing-like.
73. Anteromedial process. (0) absent; (1) present.
74. Extreme of posterolateral process of hyoid. (0) acute; (1) rounded expansion; (2) expanded, posterior border concave.
75. Origin of posterolateral process of hyoid. (0) differentiated from the posterior 1/3 of the hyale body; (1) differentiated from 1/2 of the hyale body.
76. Shape of posteromedial process of hyoid. (0) distal end expanded; (1) uniform width.
77. Intercotylar region. (0) concave; (1) straight; (2) convex. This character was treated as additive.
78. Neural spine of vertebrae I–V. (0) absent; (1) not imbricate; (2) imbricate.
79. Omosternum. (0) rounded and single; (1) distinctly bifid or divided.
80. Xiphisternum. (0) trapezoidal or semicircular; (1) V-shaped; (2) double; (3) inverted U-shaped; (4) sub-rectangular; (5) mineralized and quadrangular anterior region, with two posterior cartilaginous projections.
81. Posterior half of mesosternum. (0) uniform width; (1) expanded, but markedly narrower than the anterior extreme; (2) almost as expanded as the anterior extreme; (3) bifid.
82. Mesosternum. (0) present, Y-shaped; (1) absent, only xiphisternum.
83. Number of prepollex segments. (0) proximal element (base) plus 4 segments; (1) proximal element (base) plus 3 segments; (2) proximal element (base) plus 2 segments; (3) proximal element (base) plus 1 segment.
84. Number of carpal elements. (0) five; (1) six.
85. *Crista humeralis* in males. (0) present; (1) absent.
86. Terminal phalanges. (0) rounded or knobbed; (1) rounded and bifurcated: dilated with a split that defines two lobules; (2) T-shaped.
88. Urostyle. Flattened (0); of cylindrical section (1).

Characters of larval Chondrocranium (after Larson and de Sá 1998)
89. Ventromedial fusion of *suprarostral corpus*. (0) absent; (1) present.
90. Relationship between *suprarostral corpus* and ala. (0) not fused; (1) fused; (2) ventrally fused.
91. *Planum trabeculare anticum*. (0) wide; (1) narrow.
92. Frontoparietal fenestra. (0) open throughout its length; (1) posterior half closed.
93. *Processus anterolateralis* of *crista parotica*. (0) small and triangular; (1) large and triangular; (2) long finger-like projection; (3) large and rectangular; (4) absent.
94. Posterolateral extension of the palatoquadrate. (0) does not reach the level of attachment of *processus ascendens* to the braincase; (1) reaches the level of attachment of the *processus ascendens* to the braincase; (2) extends beyond the level of attachment of the processus ascendens to the braincase; (3) extends beyond the anterior margin of otic capsules; (4) reaches 1/3 the length of the otic capsule.
95. Attachment of the *processus ascendens*. (0) low; (1) intermediate.
96. *Processus pseudoterygoideus*. (0) absent; (1) present.
97. *Pars articularis quadrati*. (0) distinct from *processus muscularis*, in lateral view; (1) indistinct from *processus muscularis*; when the *processus muscularis* is wide, it is almost impossible to distinguish the *pars articularis quadrati* in lateral view. It is one of the two distinctive anterior processes that bear the palatoquadrate. Another one is the *processus muscularis quadrati*, which is broad, flat, and extends dorsally from the lateral margin of the palatoquadrate at a level just posterior to the *pars articularis quadrati*.
98. *Processus muscularis*. (0) large; (1) reduced.
99. *Commissura quadratoorbitalis*. (0) absent; (1) present.
100. *Processus anterolateralis hyalis*. (0) absent; (1) present.
101. Anterior process of hypobranchial plate. (0) absent; (1) present.
102. *Processus branchialis*. (0) open, without cartilaginous bridge between Ceratobranchials II and III; (1) closed, with a distinctive cartilaginous bridge between Ceratobranchials II and III.
103. Dorsal curvature of the posterior margin of the palatoquadrate. (0) present; (1) absent.
104. *Hyoquadrate process*. (0) small and triangular in lateral view; (1) large and rounded in lateral view.